BEERAVALLI, LAKSHMI P, Ph.D. Response of Pulmonary and Cardiac Cells to Ceria Nanoparticle Exposure. (2020)
Directed by Joseph M Starobin. 90pp.

Respiratory diseases due to penetration of ultra-fine particles are increasing at a steady rate. The main portal of entries for such particles is a gas-exchange region of the lung which has large absorption area with a thin alveolo-capillary barrier. The goal of this work is to develop this barrier and determine the toxic effects of cerium dioxide nanoparticles exposure on the developed barrier *in-vitro*. As a part of preliminary assessment, we aimed at investigating the *in-vitro* toxic effects of 15-30nm nanoceria on A549 epithelial cell line and EA.hy926 endothelial cell line monocultures. We determined cytotoxicity using membrane integrity and oxidative stress using reactive oxygen species assays. Cellular toxicity was analyzed using confocal microscopy.

The A549 and EA.hy926 cell lines were cultured on either side of a permeable transwell insert to establish the co-culture and to mimic the complex 3D- structure of alveolo-capillary barrier. We found that A549 cells failed to form the tight junctions necessary for forming a functional barrier *in-vitro*, therefore we treated them with dexamethasone. Dexamethasone helped to form the tight junctions which was confirmed by using Confocal Microscopy and barrier electrical resistance measurements. A549 epithelial cells cultured on the apical side of the transwell insert were incubated with cerium dioxide nanoparticles for 24, 48 and 72 hours to reproduce the physiological environment with supply of nutrients

from basal side and the apical pole of the cells exposed to air i.e., experiments were conducted on air liquid interface and under submerged conditions. The transport of cerium dioxide nanoparticles across the alveolo-capillary barrier was analyzed by assessing the changes in the barrier resistance measurements.

We also determined the transfer of cerium dioxide nanoparticles along with the inhaled oxygen across the alveolo-capillary barrier in healthy and diseased individuals using in-silico modeling method using reaction-diffusion model. The obtained oxygen transfer values were further used to monitor the changes in the cardiac cells of healthy and diseased individuals using Fick's law, focusing on effects in cardiac output, oxygen consumption, blood transport in arteries and veins.

In summary, the experiments demonstrated that our co-culture system provides a suitable *in-vitro* model to examine the effects of nanoparticles on the alveolo-capillary barrier and to investigate the mechanism of particulate matter toxicity across this functional barrier.

RESPONSE OF PULMONARY AND CARDIAC CELLS TO CERIA NANOPARTICLE EXPOSURE

by

Lakshmi P Beeravalli

A Dissertation Submitted to
the Faculty of The Graduate School at
The University of North Carolina at Greensboro
in Partial Fulfillment
of the Requirements for the Degree
Doctor of Philosophy

Greensboro
2020

Approved by

_____

Committee Chair

APPROVAL PAGE

This dissertation written by Lakshmi P Beeravalli has been approved by the following committee of the Faculty of The Graduate School at The University of North Carolina at Greensboro.

Committee Chair _____
Joseph M Starobin

Committee Members _____
Shyam Aravamudhan

_____
Dennis R LaJeunesse

_____
Tetyana Ignatova

_____
Date of Acceptance by Committee

_____
Date of Final Oral Examination

TABLE OF CONTENTS

Page

LIST OF TABLES

Page

LIST OF FIGURES

Page

CHAPTER I
INTRODUCTION

1.1.Background and Significance

There is an enormous increase in the usage of engineered nanoparticles in recent years. Due to the scalable properties of the nanoparticles, many new products are being created which led to the involvement of the regulatory bodies for the responsible usage of the products. EU regulations has announced a regulatory legislation in September 2017 for the safety evaluation of the nanomaterials while in US, the regulations are taken by Food and Drug Administration (FDA) for the better research implementations surrounding safety concerns[1]. This knocked down the usage of nanoparticles making toxicity a major concern.

Cerium dioxide nanoparticles (CeO_2) used in this study are the metal oxide nanoparticles which are widely used in cosmetics, as diesel fuel additives, sunscreens, in semi-conductor industry etc. Cerium dioxide nanoparticles are majorly used as the diesel fuel additives or fuel catalysts in automobile industry based on their ability to reduce the soot and increase the combustion fuel efficiency. However, the engine tests have reported that cerium dioxide nanoparticles of <100nm have been emitted in the exhaust[2]. The main route of exposure to humans in such case is inhalation. Taking this into consideration, this dissertation focuses on the toxicity assessment of CeO_2 nanoparticles on the pulmonary

and cardiac cells, based on its application as diesel fuel additive. The released CeO_2 nanoparticles from the emissions might get deposited on the skin or inhaled. As inhalation is the main route of exposure and major portal of entry to these extremely small sized nanoparticles, the inhalation route of exposure will be focused. Studies done by Oberdorster et al., have shown the particle size dependent deposition and penetration in various parts of the pulmonary region[3, 4]. In their study, the particles in the range of 15-20nm have reported to enter the alveolar region. Cerium dioxide nanoparticles have poor solubility and can aggregate deeper in the alveolar region and if not cleared from the body, they may enter the systemic circulation through the air-blood barrier. Clearance mechanisms which activate after the entry of the nanoparticles like the physical and chemical translocations proved to be ineffective in clearing out the fine particles. Nanoparticles tend to aggregate in different organs if they are not cleared from the body which lead to many toxicities and diseases[5]. Certain theories states that toxicity and dispersion are inter-related[6, 7]. As mentioned earlier inhalation is the main route of exposure for cerium dioxide nanoparticles released into emission exhausts, hence it is necessary to study the effects related to dispersion ability of these inhaled particles as they tend to increase the lung inflammation and oxidative stress in pulmonary cells.

Apart from dispersion, there are also other properties which tend to induce toxicity at a certain level in different organs of the body. These include size, shape, concentration, cell type, surface charge and coating. These properties affected people with dermal toxicity and cardiac toxicity[8].

Oral exposure did not induce toxicity in many cases hence it is not a major toxicity route for ceria nanoparticles. Inhalation remains the major route of toxic exposure to these nanoparticles being released as air borne particles into the environment, they have poor solubility as air borne particles and hence toxicity assessment in terms of dispersion should be checked. The ECHA database reported the ceria nanoparticle toxic inhalation exposure in workers as $3mg/m^3$ and $1.5mg/m^3$ in general population. Studies have not yet been conducted on determining the toxicity of ceria nanoparticles at these reported concentrations in an *in-vitro* setup.

Previous studies indicated the effects of cerium dioxide nanoparticles on the in-vitro alveolo-capillary barrier at varied concentration. This dissertation focused on performing the exposure studies not only through varied concentrations but also focused on the reported ECHA mentioned industrially exposed concentrations.

Exposure through inhalation will also require toxicity studies to be done based on the dispersion states to determine the dispersibility and solubility states hence a comparative study has been done using tween-80 and complete media.

Thus, we aimed at developing the functional barrier and studied the effects of CeO_2 nanoparticles on the developed barrier in-vitro. This barrier should be very tight and is termed as a gas-exchange region.

Further using in-silico method, we determined the effects on the transfer of oxygen along when exposed to CeO_2 nanoparticles.

1.2. Hypothesis and Aims

The central hypothesis of the dissertation states that cerium dioxide nanoparticles reduce the viability of the pulmonary cells based on their dispersion ability and penetrate the air-blood barrier causing harm to the cardiac cells.

The major aim is to test the viability of pulmonary A549 epithelial and EA.hy926 endothelial cells which form the physiological alveolo-capillary barrier on exposure to cerium dioxide nanoparticles with the focus on the diesel fuel additive application-based toxicity through preliminary cytotoxicity analysis, confocal microscopy and TEER (transepithelial/endothelial resistance) measurements.

This dissertation also aims at testing the hypothesis that cerium dioxide nanoparticles toxicity is dependent upon dispersion property in the cells owing to their poor solubility as air-borne particles.

The specific aims are as follows:

1) Specific aim 1: Determine the toxicity of cerium dioxide nanoparticles on pulmonary epithelial and endothelial cells
2) Specific aim 2: Model and determine the effects of cerium dioxide nanoparticles on oxygen transfer and on cardiac cells using in-silico methods
3) Specific aim 3: Determine conditions for the development of functional cellular junctions and the formation of tight air-blood barrier to that observed in-vivo.

1.3. Nanotechnology and Engineered Nanoparticles

Nanotechnology is a major advancement in science, owing to its ability to manipulate matter on a molecular and atomic scale. This modern nanoscale science aids in design and synthesis by altering the size and shape of various materials in building new structures termed nano-objects like nanoparticles, nanoplates and nanofibers.

The particle shaped nano-objects are termed as nanoparticles. According to the International Organization for Standardization (ISO), a nanoparticle is defined as a non-object containing all the three dimensions in nanoscale ranging from 1 to 100nm. The greater interest in the nanoparticles comes from their tunable physical, chemical and biological properties.

Nanoparticles are categorized into different types based on their origin, dimension and source. Based on the source, the nanoparticles are categorized into incidental and engineered nanoparticles. Details on engineered nanoparticles will only be discussed further in this document giving importance to CeO_2 nanoparticles used in the study.

Engineered nanoparticles are manufactured by humans to have certain properties for desired applications. These nanoparticles are used in cosmetics, tires, sunscreens, food additives etc. Metal oxide nanoparticles are one of the major categories belonging to engineered nanoparticles. These are considered to be one of the most important materials which are industrially manufactured and produced in large amounts and used widely, having many applications in industry, medicine and ecosystem. Few of the many metal oxide nanoparticles used for various commercial applications include zinc oxide, titanium dioxide, cerium dioxide (CeO_2), etc.[9]. Due to the enhanced usage of the nanoparticles,

concerns relating to their toxicity gained much importance which aimed at involvement of an active research on nanoparticles in the field of nanotoxicology. Apart from many applications, many studies have been reported in the recent years that nanoparticles are harmful to the body.

1.4. Cerium Dioxide (CeO_2 Nanoparticles): Use as Fuel Additives

Cerium(Ce) belongs to the lanthanide series of the periodic table. It is a rare earth metal used extensively as oxidative catalyst, fuel additives, oxygen sensors, sunscreens, UV absorbers, solid electrolytes and semiconductor manufacturing. Cerium dioxide nanoparticles are the engineered nanoparticles which gained enormous attention over the past 10 years due to their applications in various industries. Cerium have an average concentration of 50ppm in the rare earth's crust[10]. It is a very strong oxidizing agent stabilized on reacting with oxygen ligands and exists in trivalent, Ce^{3+} and tetravalent, Ce^{4+} forms[11]. These ionic forms tend to show the toxic properties which are experimented on pulmonary epithelial and endothelial cell lines and will be discussed later in this dissertation. Few of the many CeO_2 applications include fuel borne catalysts, catalysts for automobile exhaust systems[12-14], as luminescent materials[15], abrasives for chemical-mechanical planarization[16], hybrid solar cells[12], as polishing agent for television tubes, glass mirrors, ophthalmic lenses[17-19] etc. It is also used as additive in cigarettes[2]. This dissertation focuses on the toxic details based on the CeO_2 nanoparticles usage as fuel borne catalysts since 1999. CeO_2 nanoparticles are used commercially as Envirox or Rhodia diesel additives.

Fuel additives are categorized into three main groups according to European commission report: these include, refinery or functional additives, performance additives and after-market products. Cerium dioxide belong to after-market additive category which is widely used in Europe and North America[20]. Cerium acts as a fuel catalyst in donating oxygen and assists in reducing soot from diesel exhaust thereby increasing the fuel combustion efficient and reducing emission of unburnt hydrocarbons. They have a stronger oxidizing capacity which can burn the soot collected into the particulate filters. If it is used in combination with filters, it exhibits additional properties of reducing the particulate matter and the ignition temperatures by acting as a catalyst. Regeneration of the diesel filters is one of the processes done by cerium as a fuel borne catalyst. Cerium dioxide nanoparticles are not always used along with the particulate filter and in the absence of the filter, the emission rate of the particles is higher in the exhaust[21]. Much investigation is not done on the emission of cerium dioxide nanoparticles into the environment where a study done on the commercially used cerium indicated the release of these nanoparticles in a larger size[22].

However, reports indicated the presence of added CeO_2 particles in the emissions. These nanoparticles once released into the environment can be deposited into the soil, onto the skin barriers and can be inhaled. This makes it a necessity to test for the toxic effects of the added CeO_2 nanoparticles. This dissertation focuses on in-vitro inhalation toxicity studies using A549 lung epithelial and EA.hy926 endothelial cell lines.

The fate of inhaled nanoparticle starts at the absorption of nanoparticles through the mucociliary clearance of the lungs into system circulation by crossing the physiological

alveolo-capillary barrier, thereby they deposit into different parts of the body like spleen, brain, kidney etc. (fig 1). Before crossing the alveolo-capillary barrier, the nanoparticles reach the alveolar part of the lungs, which are the pulmonary functional units. This barrier is a tight epithelial tissue and semi-permeable found at the alveolus. They contain two types of cells which are AT-I or alveolar epithelial cell type 1 and AT-II which are the surfactant producing cells. The apical part of the alveolar epithelial cells contains a layer of macrophages and the basement membrane with endothelial cells. This is the vital barrier which is a tight intercellular junction that prevents the penetration of foreign particles. As the cerium dioxide nanoparticles used in the study are of 15-30nm size, they can reach the alveoli showing increased chances for these nanoparticles to cross the barrier, as the clearance mechanism failed to eliminate the nanoparticles (discussed in further sections). Hence there is a need to study the effect of cerium dioxide nanoparticles on this functional barrier. The mechanism of transfer and toxicity in humans are aimed to understand in this dissertation using in-vitro co-culture analysis, barrier electrical measurements and in-silico analysis taking regulatory guidelines of alternative methods into consideration. The physiological conditions are mimicked in-vitro to that observed in human lung environment.

1.5. Literature Review

1.5.1. Fate of Inhaled Nanoparticles: Mechanism of Deposition and Elimination

After the nanoparticle entry into the body, their fate is determined by four mechanisms: absorption, distribution to target organs, metabolism and elimination.

Nanoparticles can enter into the body through various routes, however, inhalation and oral route via the ingestion of nanoparticles remain the prominent ones. Compared to oral route, inhalation remain more vital taking into consideration, the release of cerium dioxide nanoparticles into the emission exhaust.

The main inhalation effects are determined by four inhalation properties. These include particle characteristic based deposition and uptake into the respiratory tract, clearance mechanism, translocation and the health effects after exposure[23-25]. Lung deposition and uptake of nanoparticles are dependent on factors like size, shape, composition, solubility, surface activity and charge.

Nanoparticles enter through the outside air into nose/mouth during breathing. It flows fast through the nasopharyngeal or extra thoracic region. The nanoparticles then pass through larynx from where it enters into the lung or thoracic region. Thoracic region are the conducting airways which transmits the air deeper into the lungs. The air moves faster in the upper part of the thoracic region and as the air goes deep down into alveolar region where the air movement will become stationary[26]. This is the region where the oxygen and carbon dioxide are exchanged between air and blood (fig 1).

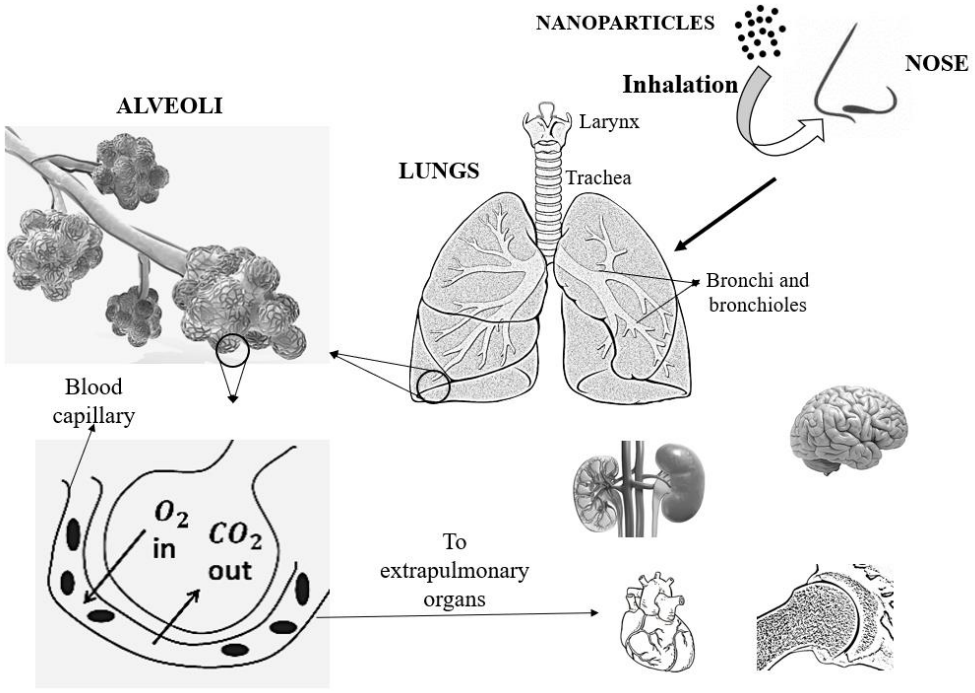

Figure 1. Nanoparticles inhalation route of exposure

Deposition of the larger micrometer sized particles are influenced by inertial impaction, gravitational settling, and interception mechanisms. However, inhaled nanoparticles are deposited by diffusion process and the rest of the mechanisms do not contribute in their deposition.

Deposition rates of the particles based on their particle size have been summarized in various studies[27, 28]; according to these studies, 80% of the inhaled 1nm or 0.001µm particles are deposited and retained in the nasopharyngeal region, 20% are deposited in the tracheobronchial region. About 50% of the 20nm sized nanoparticles are found to be deposited in the alveolo-capillary region[29-31].

There are certain clearance mechanisms in the body which help clear the deposited foreign particles thus helping in removing the toxicities. The clearance mechanisms are

chemical dissolution for the soluble nanoparticles and physical translocation for lower soluble or insoluble nanoparticles. Physical translocation of nanoparticles from one part to another part of the body is dependent on different methods based on where the nanoparticles are deposited based on their size and solubility. These include mucociliary clearance which eliminates larger size micrometer sized particles deposited in the upper part of the respiratory tract, macrophagic phagocytosis which play a primary role in removing the smaller sized nanoparticles, the other mechanisms include epithelial translocation, blood circulation and sensory neurons[32].

The nanoparticles in the range of 10-35nm are deposited in the alveoli. As the cerium dioxide nanoparticles studied in this dissertation are of the size 15-30nm, macrophage clearance mechanism will be discussed further.

Alveolar macrophages efficiency to eliminate the nanoparticles will be dependent on their ability to sense the deposited particles and on the particle size. These macrophages retain the nanoparticles for more than 700 days in humans[33]. They tend to eliminate the coarser particles at a faster rate with more efficiency[34]. However, a study conducted by Oberdorster et al., has indicated the inefficiency of macrophages in clearing the deposited titanium dioxide nanoparticles. According to their study, only about 20% of the 15-20nm sized nanoparticles were eliminated from the body, 80nm clearance was around 29%, the micrometer sized particles were cleared over 80%[35].

There are also studies which indicated a rapid translocation of deposited nanoparticles into the blood followed by translocation into various extra-pulmonary organs, from the alveoli when the macrophages failed to eliminate the foreign particles.

Nemmar et al., in their experiments with hamsters have found that the 20nm sized nanoparticles are found in blood in 5 minutes[36]. Their group also studied the translocation of radioactive labeled ultra-fine carbon particles in blood of humans after 1 minute[37]. A high proportion of carbon particles which were deposited in rat lungs were found in liver after 24-hour exposure[38]. All these studies indicate the importance of studying the toxicity in terms of dispersion in relation to deposition and the translocation into systemic circulation.

1.5.2. Toxicity of Cerium Dioxide Nanoparticles

Nanotoxicology is the field of science which helps in determining the threats posed by the nanoparticles to humans and environment by estimating their toxic effects. The assessment becomes more difficult and uncertain as the nanoparticle's scales almost becomes equal to DNA and many biological reactors inside the human body.

Due to their extremely small size, nanoparticles are more benign as they have the ability to enter the cells, translocate into different organs by penetrating the physiological barriers, interfere with the cell functions and influence the basic cellular processes like metabolism and ultimately cause death.

Cerium dioxide nanoparticles tend to aggregate within the respiratory tract and the alveoli due to their poor solubility in the biological media. Once they reach the alveoli, they can penetrate the air-blood barrier and enter the circulatory system exhibiting potential harm to heart and other vital organs of the body by disrupting the cellular processes. Cerium dioxide nanoparticle toxicity is found to be cell type dependent and the toxicity has found to increase in a dose dependent manner. Park et al., reported oxidative BEAS-2B epithelial

lung cell death on exposure to 20µg/ml concentration of Cerium dioxide nanoparticles after 36 hours of exposure[39].

Cerium dioxide nanoparticles through inhalation exposure will enter into the respiratory tract, move through the alveoli, penetrate the air-blood barrier, enter into the circulatory system exerting toxic effects to vital organs of the body. Although CeO_2 have many applications, many other studies indicated the toxic effects. The live animal studies like those conducted in rats have shown the pulmonary fibrosis, hepatic toxicity and loss of alveolar macrophage function in rats after intratracheal instillation[40]. These nanoparticles tend to aggregate because of the weak vanderwaals forces or the stronger covalent bonds.

Cerium dioxide nanoparticles toxicity is based on various physicochemical properties like size, morphology, cell type, dispersion etc.(fig 2). Among these properties, toxicity due to inhalation exposure will result from dispersion state of the nanoparticles as it can potentially harm the biological reactivity. We have done experiments using tween-80 for evenly distributing the nanoparticles and did a comparative study with those in the aggregated forms. The aggregated and non-aggregated forms were confirmed using Dynamic Light Scattering and Zeta potential studies, details on the toxicity will be discussed in chapter 2.

Many experiments were performed on lung cells as inhalation is the main route of entry to nanoparticles. an increase in toxicity and decrease in cell viability was found in BEAS-2B cell lines following CeO_2 exposure [39]. CeO2 nanoparticles also induced oxidative stress by increasing the ROS cell levels via inducing HO-1 through Nrf2

pathway[41]. Inhaled particles are known to show an effect on cardiovascular physiology by altering the cardiac rhythm and arteries diameter. Studies also indicated the transfer of inhaled nanoparticles from respiratory barrier into the blood stream effecting cardiac cells[42, 43]. OberdÖrster et al has summarized the effects of inhaled nanoparticle dusts through their translocation on different parts of the body[33]. A study done on C. elegans exposed to CeO_2 nanoparticle aggregates inhibited their growth which shows that nano-scale ceria aggregates are toxic to living organisms[44].

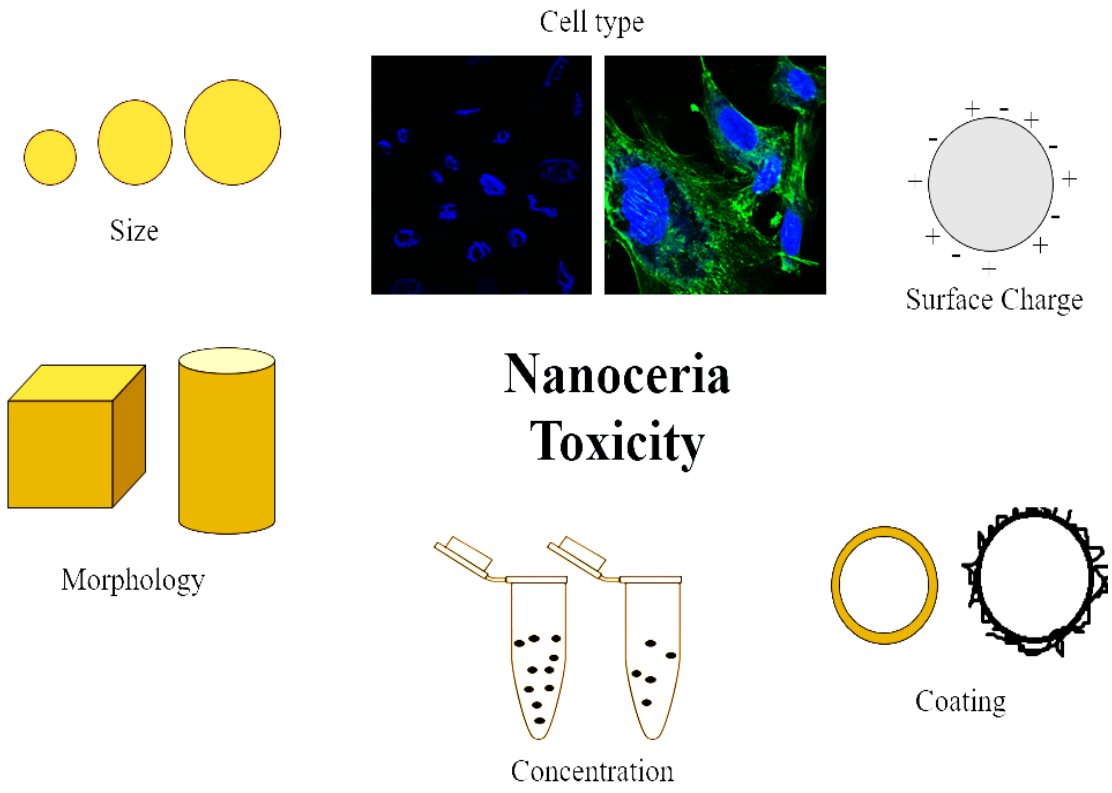

Figure 2. Physicochemical properties affecting cerium dioxide nanoparticle toxicity

Another study done by Cho et al., in 2010 reported the acute inflammatory effects of CeO_2 nanoparticles on rat lungs following instillation of better dispersed nanoparticles[45]. Lung inflammation and fibrosis has also been observed in another study done on rats by

Ma, J.Y., et al. through intratracheal exposure to CeO_2 nanoparticles[46]. In their study they also reported a damage to air-blood barrier.

1.6. In-vitro Toxicity Studies

1.6.1. Regulatory Guidelines for Safety Assessment of Nanoparticles

The US FDA has put a lot of effort in updating the regulatory guidelines in nanotechnology in enhancing the abilities of the researchers for continued nanoparticle safety assessment.

Nanoparticles used commercially should undergo safety assessment studies to be released into the market. Many harmonized regulatory guidelines from FDA and EU are in place to determine the usage of sensitive assays which can detect the lowest limit of nanoparticles taking nanoparticle properties like dispersion and solubility into consideration.

The safety data sheets (SDS) that are provided along with the products contains toxicological section (section 16) according to GHS (Globally Harmonized System of classification and labeling) guidelines. This section should include all the toxicity information in terms of LC50/median lethal concentration (for inhalation) and LD50/median lethal dose (for oral and dermal) exposures. This data will be collected from previous animal or in-vitro cell studies results listed in well-curated sources like REACH ECHA (Registration, Evaluation, Authorization and Restriction of chemicals) databases in order to reduce the usage of animals for ethical reasons.

Cerium dioxide which is marketed as diesel fuel additive have shown to contain an LC50 as 4700µm[47]. The ECHA database reported the inhalation toxic effects at a

concentration of 3mg/m^3 for workers and for general population it was found to be about 1.5 mg/m^3 (source: ECHA database, obtained using CeO_2 CAS No.).

All the regulations aim at reducing or limiting the usage of animals and focus on testing the nanoparticles using alternative methods like in-vitro studies, in-silico studies and other computational tools. OECD (Organization for Economic Cooperation and Development) for nanotechnology has implemented a regulatory framework providing guidelines to ensure safer usage of nanoparticles[48]. OECD also listed out the guidelines for testing the chemicals giving importance to alternative methods and reducing the animal usage. OECD 403 testing guidelines gives details on the acute inhalation toxicity studies (LC50)[49].

1.6.2. Monoculture, Co-culture, and Physiological Barrier Transport Studies

Innovations in the testing strategies have been made with in-vitro experiments. These experiments must be approved of performing and giving results to that observed in animal studies. Previously in-vitro tests were performed using the immortalized cell lines which were not sensitive to any engineered nanoparticles and required higher doses. These cell lines did not show accurate results in regard to obtaining the biological impact evaluation. This led to the use of primary cell cultures whose physical composition was found to be normal and advantageous in determining the effects close to that observed in-vivo.

Respiratory system is complex and vital for human body. Any pollutant entering the body will have primary route of exposure as inhalation. Hence it is important in studying the effects on respiratory system. Many in-vitro studies have been performed on

single lung cell lines either epithelial or endothelial in order to obtain prior effects through different assays.

Studies performed on single cell-line is termed as monocultures. During recent years, researchers are focusing on the co-culture methods to evaluate the transport to extra-pulmonary organs in-vitro. These 3D cultures or co-cultures will contain culturing of two cell-lines on either side of the membrane.

TEER measurements used on organ-on a chip as an integrated system has been proved to be effective in assessment of toxic effects of nanoparticles by giving the resistance values based on permeability. Many in-vitro cells models have been studied as co-culture studies under physiological conditions similar to that observed in-vivo. Hence it is important to maintain the factors like cell passage number, temperature etc., without disturbing the cell-culture environment, which might possibly affect the results if mimicked in-vivo on the semi-permeable tight junctions.

Monocultures and co-cultures were given much importance in the regulatory perspective. As inhalation toxicity is focused in the present study, the hazard evaluation for inhalation studies is more complex and more technical and is expensive if performed on animals. Animal inhalation studies if performed requires thorough OECD and EPA guidelines with a larger group of animals. Hence, human cell lines are preferred as they give much accurate and close to thorough evaluation of exposures. Another important alternate method for toxicity studies are the computational methods. The non-animal approaches follow a 3R rule which is refinement, replacement and reduction. There is a

need for a faster yet efficient replacement for animal studies which should ne versatile in simulating the human effects after exposure. These tests should be able to reproduce the findings with those done in animals/in-vivo studies.

The increased usage of co-culture as an alternate approach is due to their ability in showing a more relevant and closer resemblance to human morphology and tissue structure. In the air-blood barrier co-culture studies, barrier function and hence the mucociliary responses can be closely monitored. One of the methods to determine the barrier integrity is by measuring the electrical resistance indicating the cellular flow across the barrier. This is termed as transepithelial/endothelial electrical resistance (TEER). These values are considered to be the strong indicators in quantifying the stages of growth and differentiation of cells.

Previous in-vitro studies have focused on the usage of either epithelial or endothelial cell cultures. Cell monocultures might help in the toxicity assessment of nanoparticles to some extent, but a co-culture helps in understanding the barrier parameters, diffusion mechanism which in turn helps in giving the information on toxic nature of nanoparticles through size and concentration etc. of the nanoparticles. An in-vitro co-culture model is mentioned in figure 3. The tight junction (also termed as intercellular junction or zona occludens) formed as a result of co-culture of epithelial and endothelial cells should be able to control the transport or penetration of nanoparticles across the barrier into the systemic circulation. A qualitative visual analysis through confocal microscopy using zo-1 marker was provided in this dissertation however a quantitative analysis is also required to help understand the transcellular parameters. Hence, barrier

resistance measurements were also reported using TEER (transepithelial/endothelial resistance) analysis. TEER instrument gives the electrical resistance readings across the monolayers. TEER measurements are dependent on temperature, media formulation and passage number of the cells. These measurements were analyzed in two sections: measurements obtained directly on the final day and those obtained on the progressive alternative days. These values were reported as the confirmation of the formation of tight junctions by measuring the monolayer integrity and permeability[50].

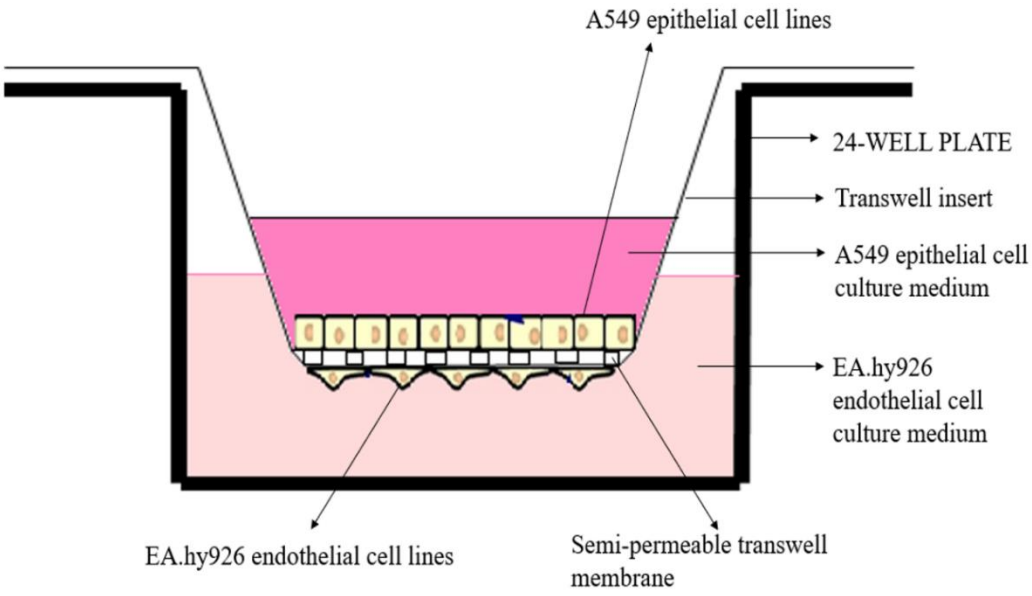

Figure 3. Modeling in-vitro alveolo-capillary barrier

1.7. Computational analysis of CeO_2 nanoparticle transfer across air-blood barrier

Respiration helps in the movement of outside air into the blood and movement of carbon dioxide from blood into the environment. If any pollutant is added to the inspired air, the effects will be affecting the system starting from lungs to the extra pulmonary

organs. In this paper, we aimed at modeling the transfer of oxygen with added cerium dioxide nanoparticles in varied concentrations through the epithelial airway and determined the effects on the volume of oxygen transfer after the cerium dioxide nanoparticle exposure using reaction-diffusion model. We also aimed at determining the effects on the cardiac output through the changes in oxygen transfer across the air-blood barrier using Fick's law and Henry's law.

The main aim of this dissertation is to computationally analyze the effects on the oxygen transfer across the air-blood barrier and determine how the changes in the volume of oxygen transfer effects the cardiac output, arterial and venous transport of oxygen after cerium dioxide nanoparticle exposure. The model used in the present study is a reaction diffusion model developed by Sebastein et al.[51]. We used this model to depict the total concentration of cerium dioxide nanoparticles along with fresh air while inhaling and relating the concentration to the changes in the quantity of the oxygen across the air-blood barrier. Fick's law and Henry's law were used to analyze further effects of the changes in oxygen concentration to the cardiac output through binding with hemoglobin[52-54].

The hypothesis is an increase in the concentration of cerium dioxide nanoparticles will lower the quantity of oxygen being transferred across the air-blood barrier due to the effects of the cerium dioxide nanoparticles on the barrier (disruption or morphological changes). We also hypothesize that any change in the oxygen transfer will affect the cardiac output, arterial and venous transport much from the normal.

There's been an increased usage of the nanoscale products over the past decade. With the increased release on the manufactured nanoscale products into the market, the regulatory framework has also made many changes in the guidelines with concerns relating to the usage of animals for the pre-market safety assessment of the engineered nanoparticles. The regulatory guidelines mandate the use of alternative approaches like in-silico methods and in-vitro methods where applicable.

One of the main reasons for the changes in the air quality is the release of various pollutants into the atmosphere. Cerium dioxide is the metal oxide and engineered nanoparticle used as fuel additive or the diesel fuel catalyst because of its ability to reduce the soot from the exhaust system. This property is mainly due to its ability in acting as a strong oxidizing agent. However, engine tests performed has shown that a small amount of these cerium dioxide nanoparticles in the ranges of below 100nm are released into the environment through particle filter in the exhaust system. The main route of entry for such nanoparticles is inhalation and ingestion to certain extent.

We focused on the inhalation route exposure effects of the cerium dioxide nanoparticles. Respiration is a term used to describe the movement of outside air into the blood (inspiration) and movement of carbon dioxide from the blood to air (expiration). This process is achieved using passive diffusion across the air-blood barrier. Air-blood barrier is a gas-exchange region which contains a border of alveoli containing an area of 100 cm^2 and each of this alveolus contains two types of epithelial cells type I and type II on the apical side and a layer of endothelial cells on the basal side. On the apical pole of the gas exchange region is the way for air through the nose, into the trachea and then deep

down into the alveoli where the exchange takes place towards the basal pole. This gas exchange region is in a width of less than a micrometer. The volume of air flow will be approximately 3L per minute. Room air will contain about 21% of the oxygen. Any change in the inhaling oxygen with pollutants will have serious effects on the extra pulmonary organs, primarily on heart. We developed in-vitro co-culture setup for the air-blood barrier mimicking the physiological conditions to that observed in a human body. Cerium dioxide nanoparticles showed an effect on this air-blood barrier. There are other reports which also indicated that nanoparticles causes an effect on the air-blood barrier[55-57]. For reconfirming the effects of these nanoparticles on air-blood barrier and to study further effects on heart, we employed the reaction-diffusion model and Fick's law.

CHAPTER II
CHARACTERIZATION OF CERIUM DIOXIDE NANOPARTICLES

The size and nature of cerium dioxide nanoparticles obtained commercially was confirmed using various characterization techniques.

2.1. Materials

Cerium dioxide nanoparticles were purchased from Nanostructured & Amorphous Materials Inc, Texas, USA with a purity of 99.9%, size 15-30nm and in powder form. Fecal calf serum and antibiotics were added to prepare A549 epithelial and EA.hy926 endothelial cell complete media. Basal media, DMEM and F-12K were obtained from ATCC. Triton-X 100 used as positive control in cell viability assays was obtained from Sigma Aldrich, MO, USA.

2.2. Particle Size Distribution Analysis Using Dynamic Light Scattering (DLS) and Zeta Potential

2.2.1. Method

Zeta potential and hydrodynamic size distribution using dynamic light scattering (DLS) of cerium dioxide nanoparticles was characterized by using Malvern ZEN3600 Zetasizer. Samples were prepared in three different vehicles at a concentration of 20mg per liter: 0.05% tween-80, A549 epithelial and EA.hy926 endothelial cell complete media.

These vehicles are used to obtain the differences in particle dispersion stability and used for analyzing particle dispersion-based cell viability assessment.

2.2.2. Results

Cerium dioxide nanoparticles obtained from the manufacturer was of 15-30nm in size and was in powder form. Dynamic light scattering data did not show the primary particle size as 15-30nm when dispersed in solutions. But when the nanoparticles were dispersed in 0.05% prepared tween-80, the particle size obtained was closer to the primary particle size with value 49.8$\pm$0.23nm and a zeta potential of -56.8mV. The poly dispersity index was found to be 0.08. The closer values are due to the ability of tween-80 in dispersing the nanoparticles uniformly.

Cerium dioxide nanoparticles were also dispersed in epithelial and endothelial complete media. The nanoparticles were found to be aggregating due to the adsorption onto the protein surfaces. The size was found to be 96.8$\pm$0.45nm and 158.63$\pm$0.28nm in epithelial and endothelial complete media respectively. The zeta potential was found to be -15.3mV and -12.9mV for epithelial and endothelial cell complete media and poly dispersity index was 0.2 and 0.5 respectively (fig 4).

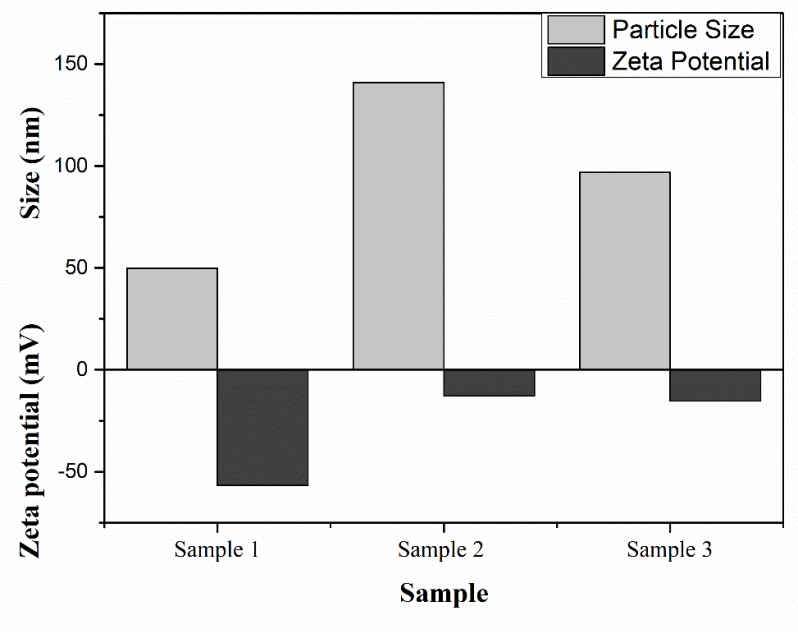

Figure 4. Size and Zeta Potential of Cerium dioxide nanoparticles: Size and zeta potential distribution of Cerium dioxide nanoparticles dispersed in 0.05% tween-80 (sample 1), DMEM complete media (sample 2) and F12-k complete media (sample 3)

2.3. Raman Spectroscopy Analysis

2.3.1. Method

Horiba XploRA Raman confocal microscope was used to obtain the raman spectra for cerium dioxide nanoparticles. Raman spectra was recorded over the range of 400-4000 cm^{-1} at room temperature.

2.3.2. Results

The structure of the sample is determined with the help of Raman spectroscopy based on vibrational modes. An intense peak at 463cm^{-1} was found to be exhibited by cerium dioxide nanoparticles and this peak was found to represent the symmetrical stretching and vibrational mode of cerium and oxygen vibrational unit (fig. 5) [58].

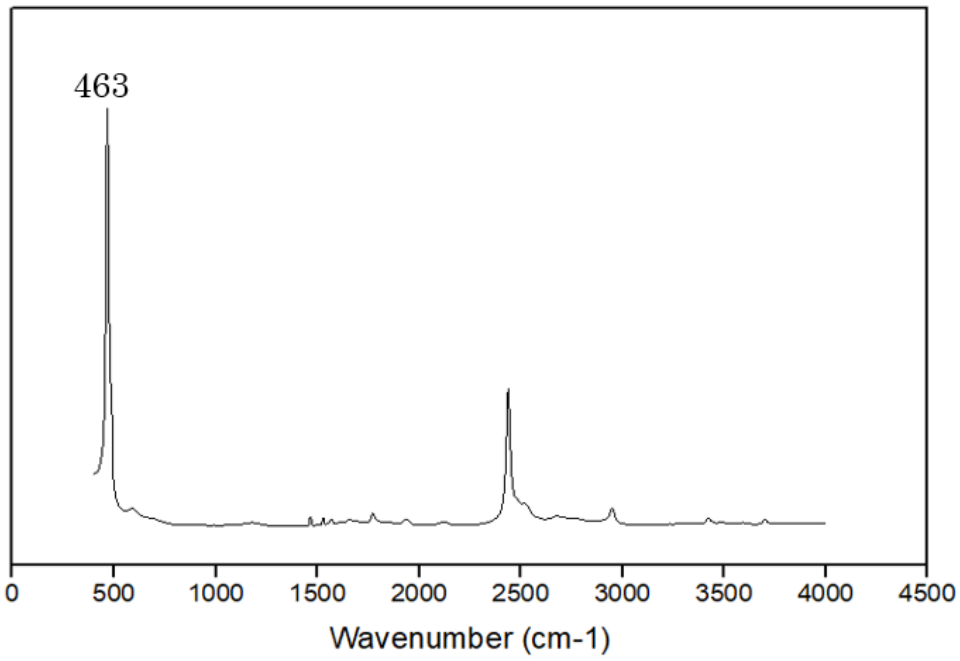

Figure 5. Raman spectroscopy of cerium dioxide nanoparticles: Raman spectroscopy peaks of 15-30nm Cerium dioxide nanoparticles shown between 400-4000cm^{-1}

2.4. X-Ray Diffraction (XRD) Analysis

2.4.1. Method

Rigaku (Agilent) Gemini XRD instrument was used to analyze the XRD spectrum of cerium dioxide nanoparticles. The spectra obtained helped in determining the phase or crystalline structures of Cerium dioxide nanoparticles. the studies were conducted, and the spectra were recorded at the room temperature.

2.4.2. Results

XRD pattern reveals the information about crystal phase and structures of cerium dioxide nanoparticle samples. The XRD pattern of Cerium dioxide nanoparticles obtained from the manufacturer is shown in figure 6. Three prominent peaks were obtained from the sample which were characteristic of cerium dioxide nanoparticles and these are [311], [220] and [111] planes which are found to have a cubic fluorite crystal structure. The results obtained were comparable to the earlier studies of literature[59].

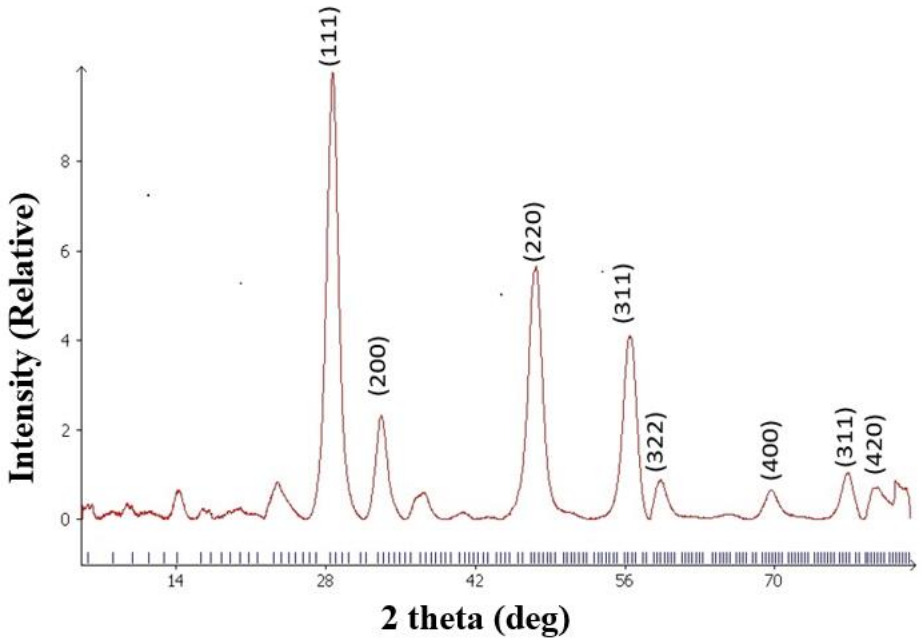

Figure 6. X-ray diffraction of Cerium dioxide nanoparticles

2.5. Fourier Transform Infrared Spectroscopy

2.5.1. Method

The characteristic FTIR absorption bands were obtained using Varian 600 Agilent FTIR with single point detector. FTIR recorded the infrared spectra in the range of 400-4000 cm^{-1}.

2.5.2. Results

The FTIR spectrum of CeO2 showed A band at 462 cm^{-1} corresponding to the Ce-O vibration was obtained from the FTIR spectrum of cerium dioxide nanoparticle sample. Another band at 1635 cm^{-1} representing the bending mode of OH group was obtained from the spectrum which might possibly be sure to the moisture residue present in the sample.

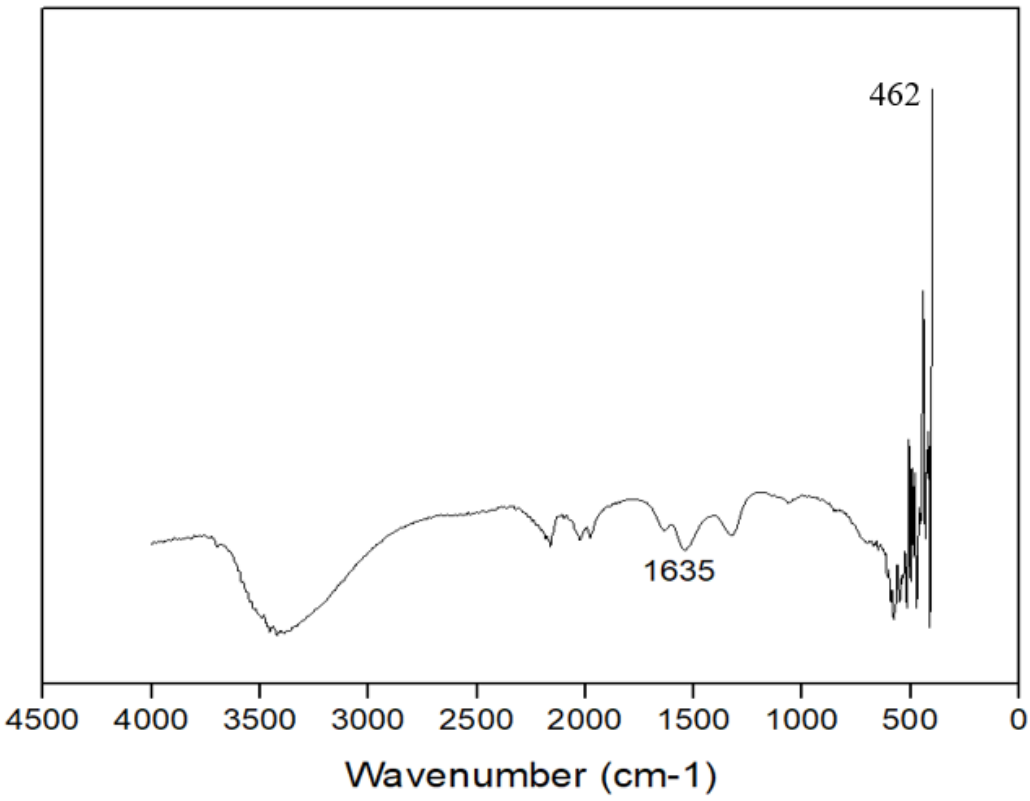

Figure 7. FTIR spectroscopy of cerium dioxide nanoparticles: FTIR spectroscopy of 15-30nm Cerium dioxide nanoparticles showing vibrational peaks corresponding dominant bands

2.6. X-ray Photoelectron Spectroscopy

2.6.1. Method

XPS helps in analyzing the possible presence of valence states and binding energies on the powder surfaces. XPS for the cerium dioxide nanoparticle sample was obtained using Thermo Scientific Escalab Xi+ (XPS/UPS/ISS/REELS).

2.6.2. Results

Ce^{3+} and Ce^{4+} are the two forms of cerium dioxide nanoparticles. XPS analysis was used to determine this ionic concentration in the sample obtained from the manufacturer. The abundance of each of these forms can also be obtained using XPS spectra. Cerium dioxide nanoparticles were found to contain an abundance of +4 form when compared to +3 form. For +4 valence form, the binding energies were found to be 883.1, 888.9, 902 and 899.4 eV whereas for +3 form, the binding energy was found to be 886.1eV. The abundance ratio presence of +3 to +4 form was found to be around 0.00699 in the sample. The data obtained through this analysis were in terms with the results found in the literature[60]. A detailed high-resolution spectrum of Cerium dioxide nanoparticles valence states with the oxygen 1s scan are shown in Figures 8, 9 and 10. A summary on the binding energy findings and the corresponding valence states for the cerium dioxide nanoparticles along with peak height, peak area and ratio values are given in table 1.

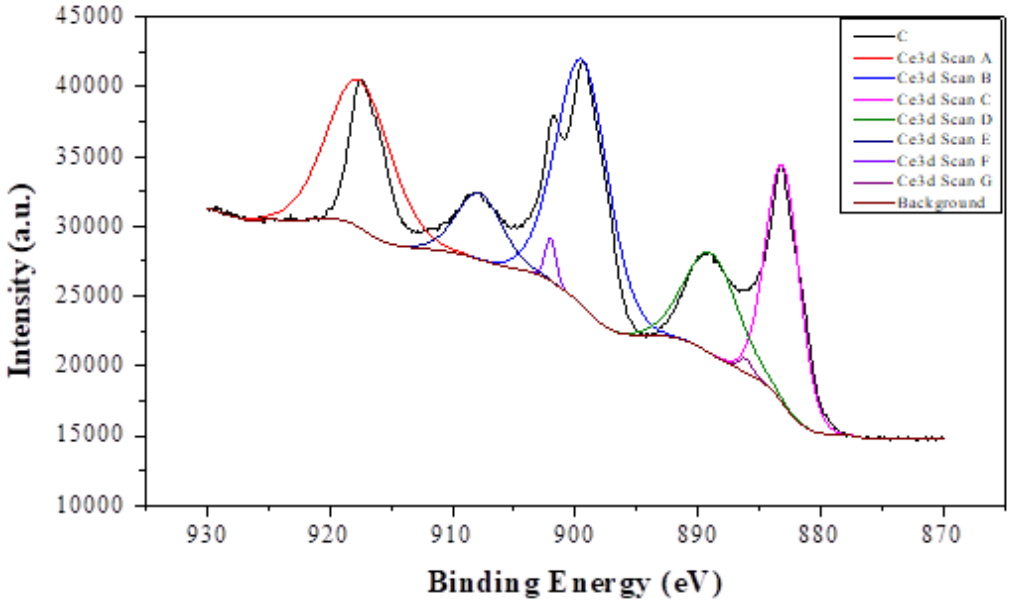

Figure 8. XPS spectrum of Cerium dioxide nanoparticles

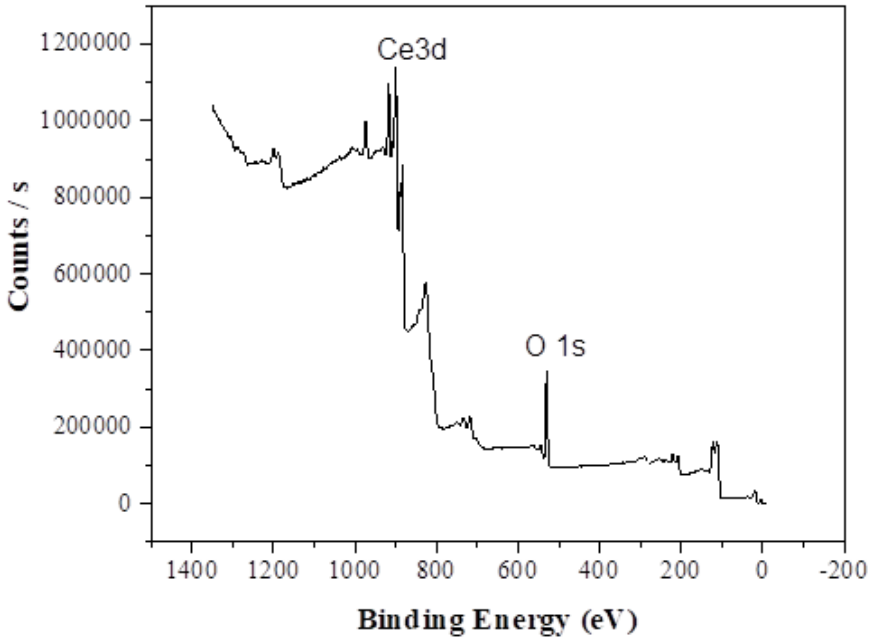

Figure 9. Wide-scan XPS survey scan spectrum of Cerium dioxide nanoparticles

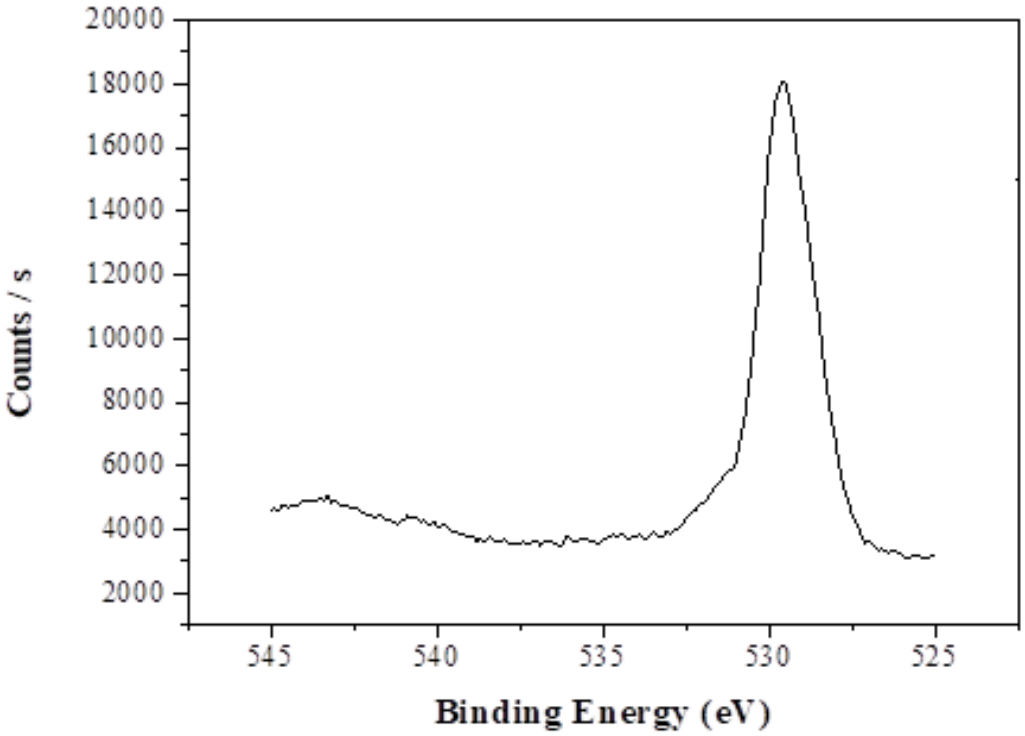

Figure 10. Oxygen 1S XPS scan of Cerium dioxide nanoparticles

Table 1. XPS characterization of Ce^{3+}/ Ce^{4+} ion concentration

Ion Characterization of CeO_2			
Valence States	**Binding energy (eV)**	**Peak height (CPS)**	**Peak area (CPS.eV)**
Ce^{3+}	886.10	991.43	1384.30
Ce^{4+}	883.10	17052.91	60058.92
Ce^{4+}	888.90	7208.06	39356.10
Ce^{4+}	899.40	17629.91	95157.27
Ce^{4+}	902.00	3091.83	3414.94

Total Peak Area (TPA)		TPA of Ce^{3+} / TPA of Ce^{4+}
Ce^{4+}	**Ce^{3+}**	
197987.23	1384.30	0.00699

CHAPTER III

BIOLOGICAL TOXICITY EVALUATION OF CERIUM DIOXIDE NANOPARTICLES

3.1.Cells, Media, and Maintenance

The lung epithelial and endothelial cell lines used in the study are A549 (CCL-185) and EA.hy926 (CRL-2922) respectively. These cell lines were obtained from ATCC. The cells were maintained by culturing in F12K media obtained from thermo-fisher scientific. The obtained media was supplemented 10% FCS and 1% PNS antibiotics. The sub-cultures were then grown in an incubator set at 37c provided with 5% carbon dioxide.

The media used for culturing and maintaining endothelial EA.hy926 cell lines is DMEM (Dulbecco's Modified Eagle Medium). DMEM media was also obtained from thermofisher scientific. This media is supplemented with 10% fetal calf serum and 1% PNS which are the antibiotics. The sub-cultures were maintained in the incubator with 37c and 5% carbon dioxide. The subcultures were maintained in T25 flasks at a density of 5000 cells per cm^2 every 2-3 days with at least 90% and above confluency.

3.2. In-vitro Viability Assays

The effects of cerium dioxide nanoparticle exposure on the A549 epithelial and EA.hy926 endothelial cell lines were assessed using the cell-viability and membrane integrity assays. The assays used include: alamar blue, lactose dehydrogenase assays.

Protocols used for these assays are shown in figure 11. The generation of free radicals were also determined using reactive oxygen species assay. The main purpose of performing these cell viability and membrane integrity assays was to determine the effects of cerium dioxide nanoparticles on the viability of A549 lung epithelial and EA.hy926 endothelial cell lines. As mentioned before, the toxicity of the cells will be primarily dependent on the dispersion property of cerium dioxide nanoparticles. Hence, a comparative cellular viability assay has been performed by dispersing the nanoparticles in epithelial and endothelial cell complete media and in tween-80 as a control study.

3.2.1. Alamar Blue Cytotoxicity Assay

For performing the alamar blue assay, epithelial and endothelial cells were cultured at a density of 3200 cell per well in a 96-well plate and allowed to grow and attach for 24hours in an incubator at 37^0c and 5% carbon dioxide. After the cells were attached, the cells were exposed to a range of concentrations of 15-30nm cerium dioxide nanoparticles for 24, 48 and 72 hours in sets of four along with positive, negative and blank as controls.

On the day of viability analysis, after exposing the cerium dioxide nanoparticles for a desired incubation period, the cells were removed from the wells, washed thrice with PBS and replaced with 100**µ**l of fresh epithelial and endothelial complete medium. To the wells with media, 10% of alamar-blue dye was added and the plates were incubated for 1-4 hours for further viability analysis. The samples were analyzed at an absorbance of 540nm and 630nm spectrophotometrically and were normalized using 630nm.

3.2.2. Lactose Dehydrogenase (LDH) Membrane Integrity Assay

A549 lung epithelial and EA.hy926 endothelial cells were cultured at a density of 3200 cells per well in a 96-well plate with a final volume of 100µl complete media. An incubation period of 24hours was given for the cells to attach. After 24hours, 50µl of cells were transferred to a new 96-well plate for further analysis. To this plate, 50µl of prepared LDH solution was added and incubated at room temperature for 30 minutes. The absorbance was measured at 490nm and 630nm after incubation, spectrophotometrically. The values were normalized using 530nm.

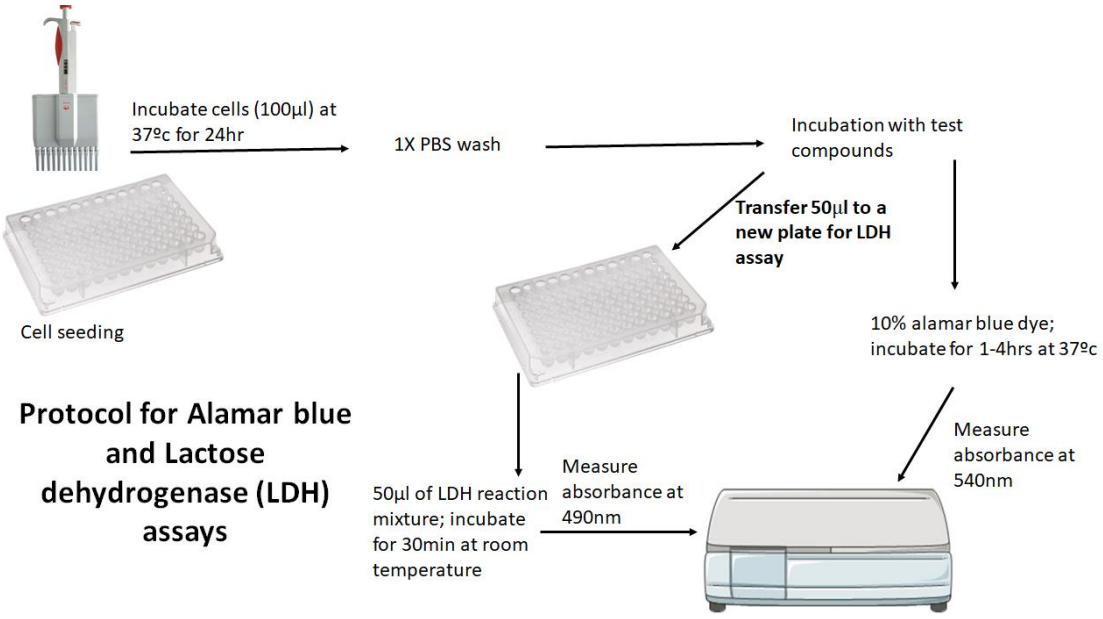

Figure 11. Experimental flow for cell-based toxicity assays: Figure showing experiment flow for alamar blue cytotoxicity assay and lactose dehydrogenase membrane integrity assay

3.2.3. Reactive Oxygen Species (ROS) Assay

Epithelial and endothelial cells were seeded at 25000 cells per well density in a 96-well plate and allowed to attach for 24hours. The media was then removed and 100µl of 1X buffer was added to the wells. The cells were then stained with 100µl per well with DCFDA solution and incubated with DCFDA solution for 45min in dark at 37c. DCFDA was removed and washed once with 1X buffer after incubation. The cells were exposed to the cerium dioxide nanoparticles in different concentrations. The plates were incubated with the nanoparticles for a period of 1h, 3h and 6h. The plates analyzed further, and readings were taken at an excitation of 485nm and an emission of 535nm spectrophotometrically. Results were determined as the change in the percent of control after background subtraction. The assay was performed for A549 epithelial and EA.hy926 cell lines individually.

3.3. Live/Dead Cell Analysis Using Confocal Microscopy

Epithelial and endothelial cells were cultured in 6-well plates on round glass coverslips at a seeding density of 0.3×10^6 cells per well. The cells were incubated to attach for 24 hours. Positive and negative controls were cultured with and without cells. The cells were then treated with 100µg/ml of cerium dioxide nanoparticles for 24hours. After exposure, the treated coverslips were removed, washed thrice with 1X PBS and fixed, followed by permeabilizing and blocking. After blocking, staining was done using actin green 488 and Nublue dyes for cytoskeleton and nucleus staining. After staining, the coverslips were rinsed after 30 minutes to remove any excess residual dyes and visualized under confocal microscopy.

3.4. Results and Discussion

3.4.1. Cell Viability Analysis: Alamar Blue Assay

Alamar blue assay is a non-toxic assay which helps in quantitatively measuring the proliferation of cell lines. This assay was performed individually on A549 lung epithelial and EA.hy926 endothelial cell lines. Alamar blue dye is used as an oxidation and/or reduction indicator by changing the color in response to a chemical reduction in the cell complete growth medium.

The alamar blue assay acts by determining the number of live cells on its reaction with alamar blue dye. The principle of this assay is that the reducing equivalents NADH/NADPH will be produced through the metabolism of viable cells. These reducing equivalents will pass the electrons into the intermediate electron transfer agent reducing the tetrazolium product into a soluble formazan product. This reduction process will be done only by the viable cells. However, the cell loses this ability to reduce the tetrazolium product at death. The generation of colored formazan is hence directly related to the number of viable cells present in the sample.

As mentioned above, only viable cells will be able to generate the signal hence, any decrease in the cellular function will cause a reduction in the absorbance.

In the present study, A549 epithelial and EA.hy926 cell lines were treated with the varied concentrations of cerium dioxide nanoparticles with 250µg/ml being the highest concentration. At this concentration, the cells showed the lowest number of viable cells which decreased more with the incubation period from 24 hours to 48 hours. However, as

the concentration of cerium dioxide nanoparticles is decreased, the number of viable cells did not show a change when compared to the negative control. In this experiment, both the epithelial and endothelial cell lines stopped showing the effect at the concentration of 50µg/ml of nanoparticles.

A comparative study to analyze the effects of cerium dioxide nanoparticles has been performed based on the dispersion property using complete media and 0.05% tween-80 separately. To perform this experiment, a new concentration of cerium dioxide nanoparticles had been prepared in complete media from the stock solution of nanoparticles suspended in 0.05% tween-80. Alamar blue assay has shown that the dispersions made with 0.05% tween-80 showed less effect on the epithelial and endothelial cell death compared to the cerium dioxide nanoparticle samples dispersed directly in the complete media. The reason for this may be due to the fact that the tween dispersed samples resulted in a stable dispersion confirmed by DLS analysis with no/less dispersion, whereas the nanoparticles dispersed in complete media showed aggregation. As studies indicate, more the dispersion, greater will be the cell death (Fig 12). However, in our study, we found that tween dispersed samples showed less toxicity compared to media dispersed samples. This might be because of the cerium dioxide nanoparticles surface saturation with tween upon dispersion.

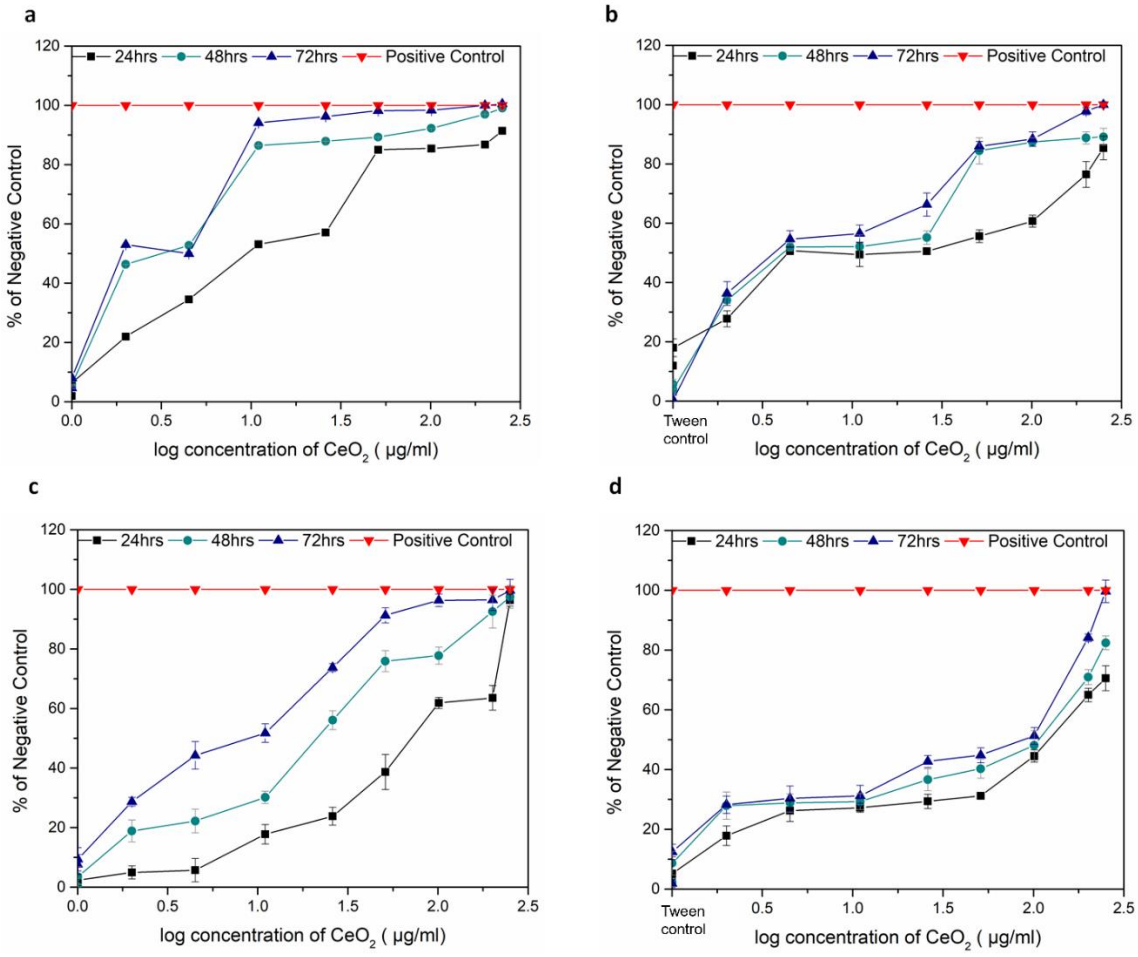

Figure 12. Alamar blue cytotoxicity assay of epithelial and endothelial cells: Alamar blue cytotoxicity assay of A549 epithelial and EA.hy926 endothelial cells at different incubation times of 24, 48 and 72hrs (a) treated with Cerium dioxide nanoparticles dispersed in A549 complete media (b) treated with Cerium dioxide nanoparticles dispersed in 0.05% tween-80 (c) treated with Cerium dioxide nanoparticles dispersed in EA.hy926 endothelial complete media, (d) treated with Cerium dioxide nanoparticles dispersed in 0.05% tween-80. Results are shown as the logarithmic graphs represented in the form of dose-response curves, presented as the mean ± standard error of the mean (n=4).

3.4.2. Cell Membrane Integrity Analysis: LDH

Lactose dehydrogenase, LDH is a soluble enzyme which is present only in the living cells. This enzyme will be released into the surrounding environment of the cells when a cell membrane is damaged due to any adverse condition. This enzyme is used as a cell death marker in the cell culture media. LDH assay is used to quantitatively measure the number of live cells and dead cells spectrophotometrically and thus the percentage of cellular cytotoxicity.

The principle of this assay is that, inside the cell LDH enzyme helps in reducing the NAD^+ to NADH and H^+ through the oxidation of lactate to pyruvate.

A catalyst termed Diaphorase helps in transferring the formed H/H^+ from NADH + H^+ to the tetrazolium salt forming a red colored formazan product. This red colored formazan product produced is directly proportional to the number of dead cells in the cell culture medium. The assay is analyzed by measuring spectrophotometrically at 490nm.

The results of LDH assay on epithelial and endothelial cell lines were comparable and in ordinance with the alamar blue assay. The dead cells were found to be higher in the epithelial and endothelial cells exposure to the cerium dioxide nanoparticles suspended in complete cell media whereas the cells treated with the nanoparticles suspended in 0.05% tween-80 showed a lower cell death (fig.13).

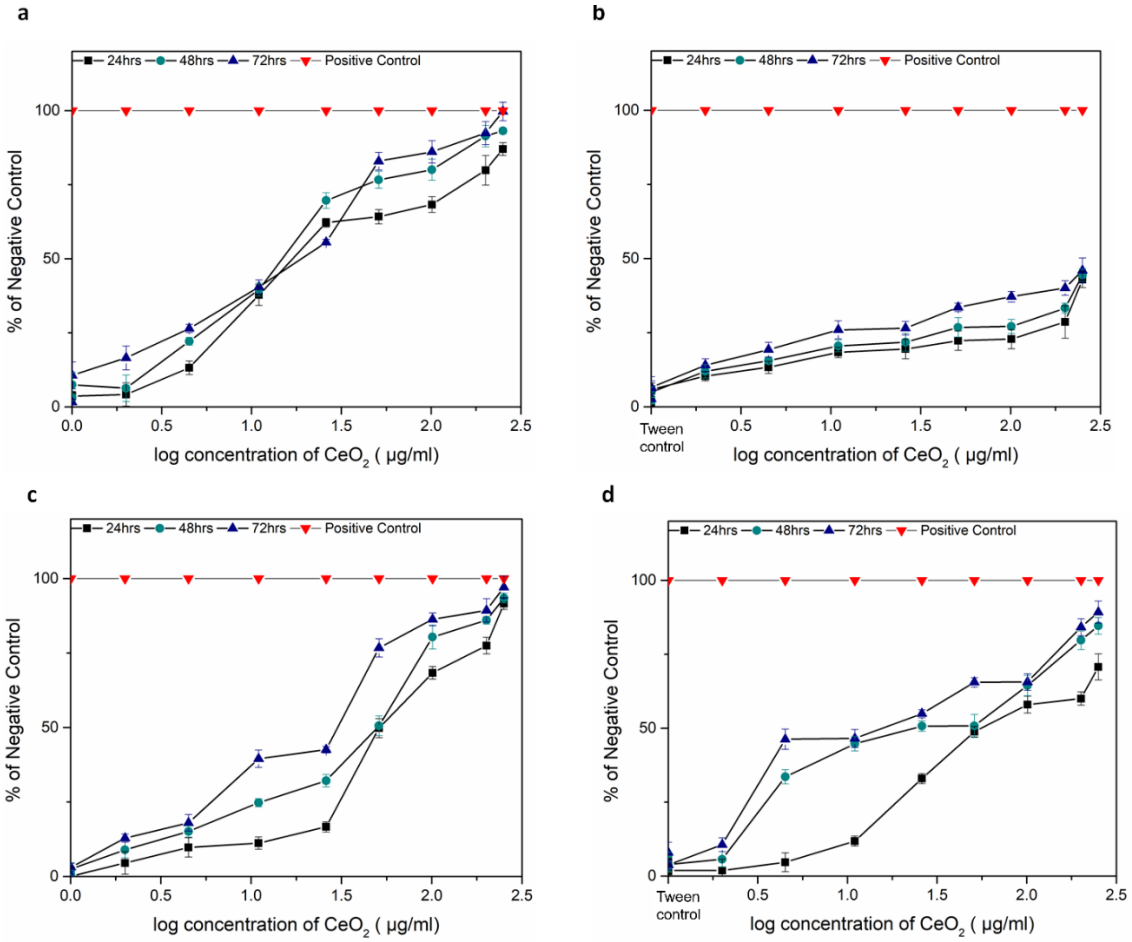

Figure 13. Lactose dehydrogenase membrane integrity assay of epithelial and endothelial cells: Lactose dehydrogenase membrane integrity assay of A549 epithelial and EA.hy926 endothelial cell lines, at different incubation times, 24hrs, 48hrs, 72hrs a) treated with Cerium dioxide nanoparticles dispersed in A549 complete media b) treated with Cerium dioxide nanoparticles dispersed in 0.05% tween-80 c) treated with Cerium dioxide nanoparticles dispersed in EA.hy926 complete media d) treated with Cerium dioxide nanoparticles dispersed in 0.05% tween-80. Results are shown as the logarithmic graphs represented in the form of dose-response curves, presented as the mean±standard error of the mean (n=4).

A comparative cell viability results between the cerium dioxide nanoparticles dispersed in cell complete media and in 0.05% tween-80 are shown in table 2: for incubation period of 24 hours. As shown in the graphs, a similar trend in the epithelial and endothelial cell lines has been observed during other incubation periods of 48 hours and 72 hours for varied concentrations of cerium dioxide nanoparticles.

Table 2. Cell viability (calculated as % negative control) comparison between Cerium dioxide nanoparticles dispersed in complete media vs 0.05 tween-80

Cell lines	Assays	Concentration (µg/ml)	Complete media	0.05% tween 80
A549 epithelial cells	a. Alamar blue	250	91.43	85.37
		100	85.45	60.69
		50	85.05	55.63
	b. Lactose dehydrogenase	250	87.03	42.94
		100	68.3	22.85
		50	64.24	22.29
EA. hy926 endothelial cells	a. Alamar blue	250	96.37	70.57
		100	61.88	44.54
		50	38.71	31.16
	b. Lactose dehydrogenase	250	91.64	70.74
		100	68.38	57.99
		50	49.78	48.82

3.4.3. Cellular Oxidative Stress Analysis: Reactive Oxygen Species (ROS):

Cerium dioxide exists in two valence forms. These include +3 and +4 oxidation or valence states. The cerium dioxide nanoparticles obtained from the manufacturer has shown to contain both the valence states confirmed using XPS analysis discussed in chapter 2. These valence states will allow the nanoparticles to store and release the oxygen molecules creating radicals. Any difference in the ratio of the valence states will create an effect on the cell lines and hence there is a need to determine the production of free radicals in the cells.

Oxidative stress is related to a production of reactive oxygen species in the cells. Increase in the reactive oxygen species will induce oxidative stress and ultimately lead to cell death. The free radicals and other reactive species are important in performing vital mechanisms inside the body if they are present in required beneficial quantities by producing enzymatic effects. However, if the levels are increased than normal, they might cause adverse changes in the cellular mechanisms and damage the cellular constituents like proteins and DNA.

This experiment helps in detecting the levels of reactive oxygen species and the superoxide's in the live epithelial and endothelial cells. An increase in the ROS production was found in a time and concentration dependent manner when compared to the negative control, which showed that the cerium dioxide nanoparticles induced oxidative stress and hence the cell death (fig.14).

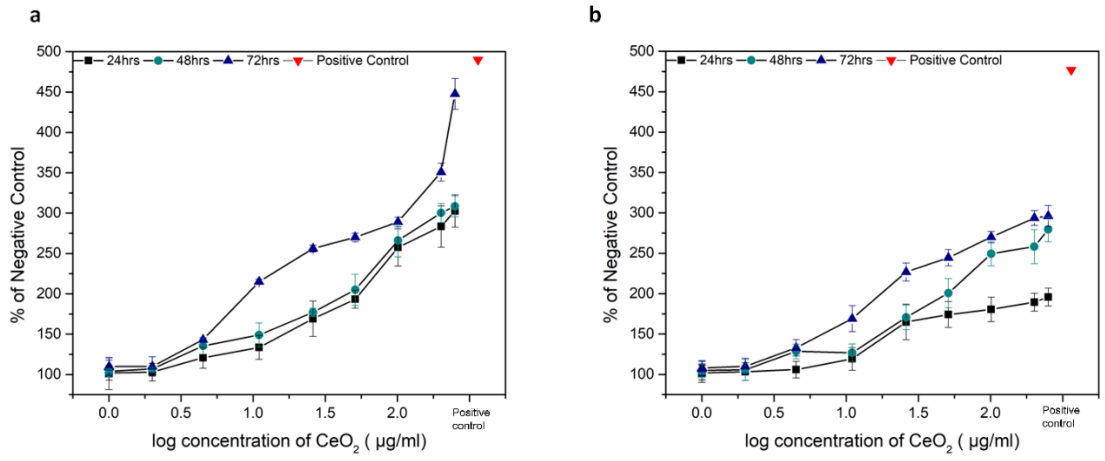

Figure 14. Reactive Oxygen Species generation assay of epithelial and endothelial cells: (a) percentage ROS production of A549 epithelial cells on exposure to varied concentrations of cerium dioxide nanoparticles (b) percentage of ROS production of EA.hy926 endothelial cell lines on exposure to Cerium dioxide nanoparticles.

3.4.4. Confocal Microscopy for Live/Dead Cell Estimation

The cellular cytotoxicity, membrane integrity and Reactive oxygen species assays have shown toxic effects of cerium dioxide nanoparticles quantitatively. However, in order to visually understand the effects, we performed the live/dead cell studies using confocal microscopy. We chose 100µg/ml cerium dioxide nanoparticle concentration from the previous result analysis to treat the A549 epithelial and EA.hy926 endothelial cell lines to determine the number for viable cells. As a positive control, triton-x 100 has been added to kill the cells and cells were grown in complete media without any exposure conditions with the test samples to be used as negative control. In ordinance with the previous assays performed, the cerium dioxide nanoparticles have shown an increased epithelial and endothelial cell death showing a reduction in the number of live cells compared to the

control and also shown a change in the morphology (fig.15). Quantitative analysis was also determined by counting the number of live A549 epithelial and EA.hy926 endothelial cells per field of view using ImageJ software (table 3).

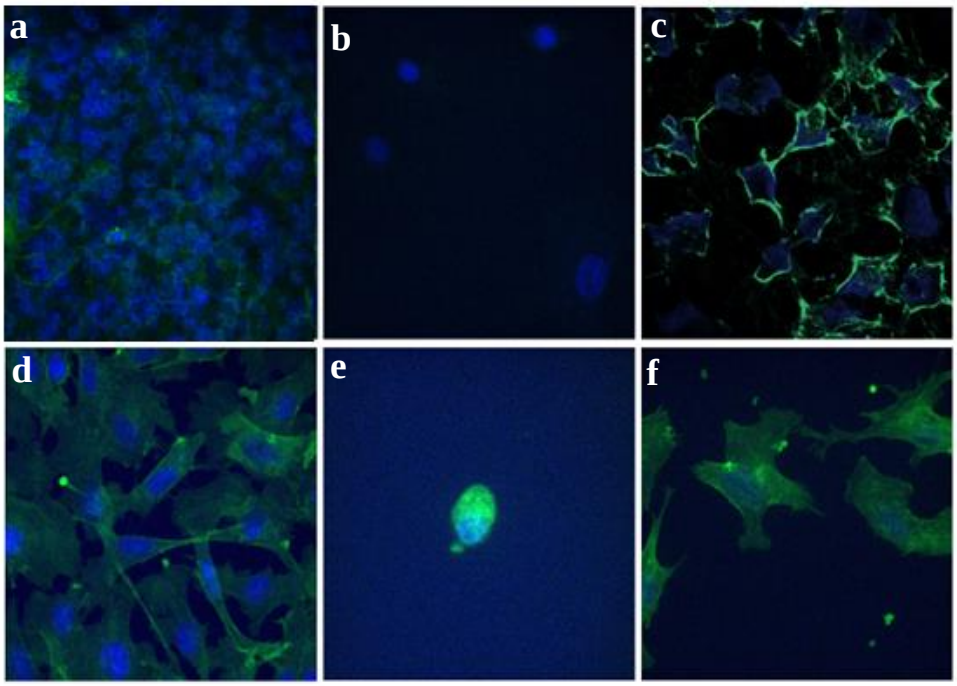

Figure 15. Cellular toxicity analysis of epithelial and endothelial cells using confocal microscopy: Confocal microscopy images of A549 and EA.hy926 cell line after treatment with 100µg/ml cerium dioxide nanoparticles. Images were taken under 60x magnification: a)A549 epithelial cell lines negative control b) A549 epithelial cell lines positive control c) A549 epithelial cell lines treated with 100µg/ml cerium dioxide nanoparticles d)Ea.hy926 endothelial cell lines negative control e) Ea.hy926 endothelial cell lines positive control f) Ea.hy926 endothelial cell lines treated with 100µg/ml cerium dioxide nanoparticles

Table 3. Live cell count for A549 epithelial and EA.hy926 endothelial cell lines treated with cerium dioxide nanoparticles

Cell lines	Controls/treated	Live cell count per field of view
A549 Epithelial cell lines	Negative control	32
	Positive control	4
	Treatment with 100µg/ml Cerium dioxide nanoparticles	4
EA.hy926 endothelial cell lines	Negative control	20
	Positive control	1
	Treatment with 100µg/ml Cerium dioxide nanoparticles	2

CHAPTER IV

IN-SILICO MODELING OF ALVEOLO-CAPILLARY BARRIER TO DETERMINE OXYGEN TRANSFER

4.1. Modeling Methods

4.1.1. Reaction-Diffusion Model

The following model is developed to explain the effects on the volume of the oxygen transferred across the air-blood barrier after cerium dioxide nanoparticle treatment:

According to this model, the lung is considered as an empty balloon with volume V, with uniform oxygen concentration, $c°$ to which we added the cerium dioxide nanoparticles represented in this model as c_1 . In general, the amount of oxygen is given as cV.

During inhalation, the oxygen rate which enters the lung (balloon) is given as $c°V>0$, where $c°$ is the oxygen in clean air with a value of 0.2.

During expiration, oxygen will be exhaled and is given as $c°V<0$.

The movement of oxygen into the lung (balloon) is expressed as follows. This reaction-diffusion model developed by Sebastein et al.,[51] is built on the following equation. Q is the diffusive part of the equation and in this process, it denotes the passive

diffusion of oxygen from deeper part of the lungs across the air-blood barrier. The rest of the equation is given as a reactive model.

$$\frac{d}{dt}(cV) = H(\dot{V})c°\dot{V} + (1 - H(\dot{V}))c\dot{V} - Q \quad (1)$$

Where; Q is the quantity of oxygen which diffuses onto the blood.

Here, H (.) is the Heaviside graph, which is a unit step function, which is 1.

Q is given as positive, as the effect on the quantity of oxygen transfer is determined in terms of inhalation.

Rearranging and further solving the equations:

$$\dot{c}V + \dot{V}(c - c°)H(\dot{V}) = -Q \quad (2)$$

$$Q = \dot{V}(c° - c)H(\dot{V}) - [\dot{c}V] \quad (3)$$

Integrating $\dot{c}V$ becomes zero as $\dot{c}$ is uniform oxygen concentration

$$Q = \dot{V}((c° + c_1) - c_2)H(\dot{V}) \quad (4)$$

Where, c_1 is the concentration of cerium dioxide nanoparticles used in the study, c_2 is the concentration of expired air and $H(\dot{V})$ is taken as 1.

$$Q = \dot{V}c° + (c_1 - c_2)\dot{V} \quad (5)$$

$$Q = \dot{V}(c° + c_1 - c_2) \quad (6)$$

Where, V̇ is the tidal volume which is volume of total air entering into the normal person at rest, calculated as ~450 ml/breath x 10 breath/min = 4500 ml/min, c^0= 0.2.

This tidal volume was altered in diseased individuals by changing the number of breaths in this model to monitor and assess the changes in the oxygen transfer in healthy and diseased individuals.

4.1.2. Fick's Law

We modeled oxygen transfer, Q in section 2 using $c°$ as the concentration of oxygen in clean air to be 0.2, c_1 as the concentration of cerium dioxide nanoparticles and c_2 as the concentration of expired air. The obtained Q values were used further to determine the changes in cardiac cells taking into account, cardiac output, oxygen consumption and blood transport in arteries and veins.

Cardiopulmonary system consists of the vital mechanisms which regulate the entire human body. It helps in regulating the gaseous transport to the tissues and from the tissues with a process termed as respiration. Cardiac output is defined as the driving force for the movement of gases through the blood medium provided by cardiopulmonary system which is found to be around 5L/min in a normal individual and is determined non-invasively using Fick's law.

Fick's law is developed as a non-invasive, cheap and easy to use technique to measure cardiac output for human pharmacological studies. This is a widely accepted, precide and accurate technique used by many computational analysts.

According to Fick's law, cardiac output is equal to oxygen consumption by the tissues over arterial and venous oxygen content difference. Adolf Fick has postulated that the entire oxygen taken in by inspiration is transferred through the lungs into the

bloodstream with no pure oxygen consumption by the lungs. Oxygen delivery is majorly determined by Cardiac output which is in turn dependent on heart rate and stroke volume.

Fick's law is given as:

$$Cadiac\ Output\ (CO) = \frac{VO_2}{CaO_2 - CvO_2} \quad (7)$$

Where VO_2 is the oxygen consumption by the tissues, CaO_2 is the arterial oxygen content and CvO_2 is the venous oxygen content

We obtained the volume of oxygen transfer across the air-blood barrier using the reaction-diffusion model as described in previous section. This volume of oxygen transfer has been converted in terms of fraction of inspired air which is 21% of oxygen in normal conditions using following formula as:

$$FiO_2\ \left(\frac{L}{min}\right) = \frac{FiO_2 - 21}{3} \quad (8)$$

Where FiO_2 is the fraction of inspired air

The movement of gases will occur through passive diffusion and the partial pressure in alveoli of the lungs (P_AO_2) is found to be 100 mm Hg in normal body where as in the blood going to the pulmonary capillaries termed as venous blood, the partial pressure is found to be 40 mm Hg. This difference in the partial pressue will create a gradient which helps in the movement of oxygen from the deeper part of alveoli into the blood through the air-blood barrier. This difference in the pressues is usually accounted to 10 mm Hg. For the current modeling, we determined the partial pressure of the oxygen exposed to cerium

dioxide nanoparticles in the alveolar space first and then in the arterial blood using the formula:

$$\text{Alveolar Oxygen pressure; } P_AO_2 = FiO_2 \times \left(P_{atm} - P_{H_2O}\right) - \frac{P_aCO_2}{R} \quad (9)$$

$$Arterial\ Oxygen\ (P_aO_2) = P_AO_2 - 10 \quad (10)$$

Where, P_AO_2 is the partial pressure of oxygen, P_{H_2O} is the partial pressure of water vapor, P_{atm} is the partial pressure of atmosphere, P_aCO_2 is the partial pressure of carbon dioxide and R is the respiratory quotient.

Adequate tissue oxygenation is required by a normal human body. The oxygen transferred across the air-blood barrier is transported to the heart in bound form to the hemoglobin or dissolved in plasma. The bound form of the oxygen with hemoglogin will account for about 98% where as that dissolved in plasma will account for only 2%. However while determining the oxygen content, bound and dissolved forms together should be taken into account.

Hemoglobin's role is to carry oxygen which is bound to four of its sites however not all the sites will be bound with oxygen. One gram of hemoglobin can carry 1.38 ml of oxygen, however, 0.4ml of it will be other molecules, hence for determining oxygen content only 1.34ml will be taken into consideration. This is termed as fully saturated hemoglobin. Any changes to this carrying capacity will results an adverse effect on heart. This satuation of oxygen for the arteries is given as:

$$S_aO_2 = \frac{HbO_2}{Hb+HbO_2} \quad (11)$$

Where S_aO_2 is the saturation of arterial oxygen and HbO_2 is the bound oxygen-hemoglobin (Hb). For the purpose of calculations, we considered hemoglobin to be 15gm/dL which is the content in a normal individual.

Hemoglobin and oxyhemoglobin monitoring is done by continous determination of mixed venous oxygen saturation which is SvO_2. Oxygen content in the body is usually evaluated by components like the satuartion of hemoglobin with oxygen i.e., bound form of hemobglobin and dissolved form of oxygen in plasma. The amount of oxygen which is consumed by tissues coming from the heart is termed as oxygen consumption of VO_2 which is the main determinant of arterial and venous oxygen content and then on the cardiac output. VO_2 increases during oxygen demand which usually occurs during disease conditions. Oxygen consumption (VO_2) is given as:

$$VO_2 = CO * Hb * 13.8 * (S_aO_2 - S_vO_2) \quad (12)$$

Where, CO is the cardiac output, L/min, Hb is the hemoglobin, gm/dL, 13.8 is the K-factor, S_aO_2 is the arterial oxygen saturation,

S_vO_2 is the venous oxygen saturation, which is given as:

$$S_vO_2 = S_aO_2 - \frac{VO_2}{CO*1.34*HB} \quad (13)$$

Blood oxygen content is given by either arterial blood content or the venous blood content. This total content is calculated by adding two forms of oxygen in blood which is dissolved in plasma and the bound form to hemoglobin. The dissolved oxygen content is calculated by multiplying partial pressure of venous or arterial oxygen with 0.0031. 0.0031

is a constant which is termed as the solubility coefficient for oxygen dissolved in plasma. The arterial and venous total blood oxygen content is given by:

Total oxygen content in arterial blood,

$$C_aO_2 = (CO * Hb * S_aO_2) + (0.0031 * P_aO_2) \quad (14)$$

Mixed venous oxygen content,

$$C_vO_2 = (CO * Hb * S_VO_2) + (0.0031 * P_vO_2) \quad (15)$$

The total oxygen content in the arteries and veins are highly dependent on the oxygen saturation of hemoglobin. Thus, we aim at determing the effects of the oxygen transfer with cerium dioxide nanoparticles on this total oxygen content.

The exposure effects of cerium dioxide nanoparticles were studies on healthy and diseased individual scenarios. The tidal volume has been altered by increasing or decreaing the number of breaths for diseased individual. The modeling in case of diseased individual has been done taking two cases into consideration; the lower number of breaths can be found in individuals with pulmonary obstruction whereas an increased number of breaths can be observed in indivuduals with asthma. The results obtained were compared with healthy individual scenario where the number of breaths and tidal volume are kept constant.

4.2. Results and Discussion

In our previous in-vitro study, we found an effect of cerium dioxide nanoparticles on the air-blood barrier using qualitative and quantitative techniques. However using the

in-silico analysis, we determined to study the effects of cerium dioxide nanoparticles on the air-blood barrier using reaction diffusion model developed by Sebastein et al[51].

Any effect on the air-blood barrier will result in a negative or toxic effect on the oxygen transfer and ultimately on the extra-pulmonary organs. Nanoparticles have the capability to transport and enter into any organ due to their surface area and extremely small size. Alveolar macrophages are the units which are vital in the clearance mechanism once the nanoparticles reach the deeper part of alveoli. However, macrophages were found to be inefficient in clearing the nanoparticles[61-63]. If the macrophages are not clearing the nanoparticles being deposited in the alveoli, there is a greater chance for the nanoparticles to be transported to the other organs along with oxygen. A study conducted on iron oxide nanoparticles had found to be entering into systemic circulation in 10min[64].

Firstly, we determined the effect on air-blood barrier to obtain the oxygen transfer volume using reaction-diffusion model. As we can see in the graph (fig 16), as the concentration is increasing, the quantity of oxygen that is being transferred across the air-blood barrier is getting decreased indicating that cerium dioxide nanoparticles are inducing the toxic effects on the barrier. We also calculated the quantity of oxygen transfer on the diseased individual with varied tidal volume $\dot{V}$, which is 4.5 L/min in healthy individuals having 10 breaths per min. thus we altered the number of breaths and obtained the differential $\dot{V}$ to determine the effects in diseased individual. Once we obtained the altered volume in the oxygen transfer, we studied the effects of oxygen on the heart focusing on three main determinants: cardiac output, oxygen consumption by tissues, arterial and venous oxygen blood content using Fick's law.

Figure 17 is showing the effects of oxygen transfer on the oxygen consumption by tissues. Lowest oxygen consumption is observed during low oxygen transfer as a result of cerium dioxide nanoparticle exposure, as a result of which the oxygen demand is found to be rising which is observed under abnormal conditions (figure 17b). Cardiac output has found to be least with the highest concentration of cerium dioxide nanoparticles. Cardiac output was also analyzed in healthy and diseased individuals with varied tidal volume (figure 18).

Arterial blood saturation was found to be about 95-100% whereas mixed venous blood was found to be saturated with 60-80% oxygen. This saturation percent was found to be extemely low in our study. This saturation percent will in turn effect the arterial and venous oxygen blood content, the normal arterial blood content in healthy individual was found to be 1005 mL/min whereas the venous blood oxygen content was found to be 775 mL/min. However, the differential exposure concentration of cerium dioxide nanoparticles showed an effect in arterial and venous oxygen transport in our modeling used by Fick's law. As the concentration was increased, the arterial and venous blood oxygen transport was found to be decreased and found to have deviated way much than normal values obsreved in healthy individual (figure 19).

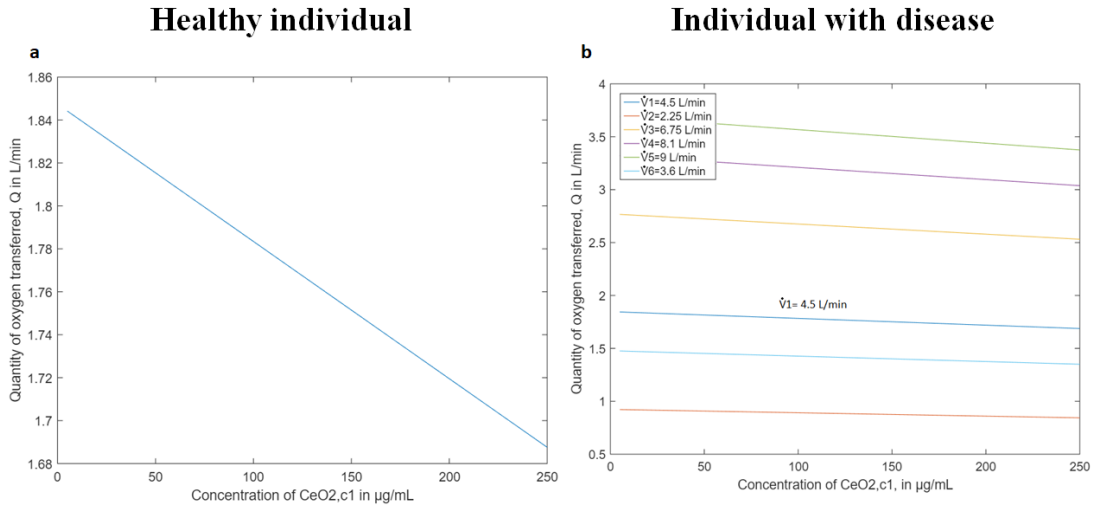

Figure 16. Effects of cerium dioxide nanoparticles on inhaled oxygen transfer: Effect of Cerium dioxide (CeO2) nanoparticles on the transfer of inhaled oxygen across the air-blood barrier using reaction-diffusion model, $\boldsymbol{Q = \dot{V}(c^{\circ} + c_1 - c_2)}$; $\boldsymbol{Q}$ is the quantity of oxygen transferred, $\boldsymbol{\dot{V}}$ is the tidal volume which is 4.5l/min in healthy individual, $\boldsymbol{c^{\circ}}$ is the oxygen concentration in clean air which is 0.2 in healthy individual, $\boldsymbol{c_1}$ is the concentration of cerium dioxide nanoparticles and $\boldsymbol{c_2}$ is the expired air: a) Graph showing the effect of CeO2 nanoparticles on oxygen transfer (Q) in healthy individual b) Graph showing effect of cerium dioxide nanoparticles on the oxygen transfer (Q) for the diseased individual with varied $\boldsymbol{\dot{V}}$, which is calculated with variations in number of breaths per minute

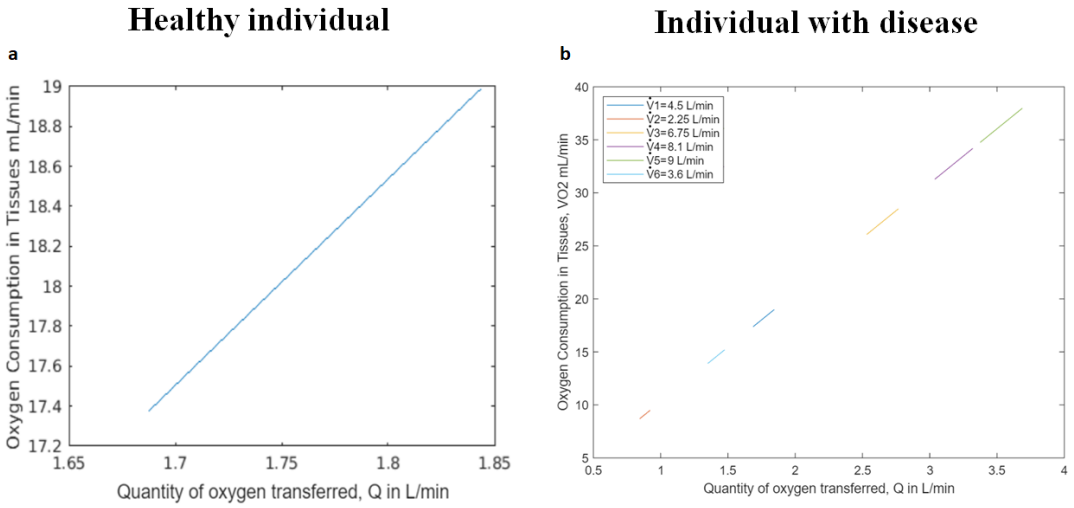

Figure 17. Effects of cerium dioxide nanoparticles on oxygen consumption: Graph showing an increase in the oxygen demand and oxygen consumption by tissues: as the amount of oxygen transfer is increasing, there is a rise in the amount of oxygen consumption by tissues which is normally observed under disease or abnormal conditions a) Graph showing the effect of CeO2 nanoparticles on oxygen consumption by tissues in healthy individual b) Graph showing effect of cerium dioxide nanoparticles on the oxygen consumption by tissues for the diseased individual with varied $\dot{V}$, which is calculated with variations in number of breaths per minute

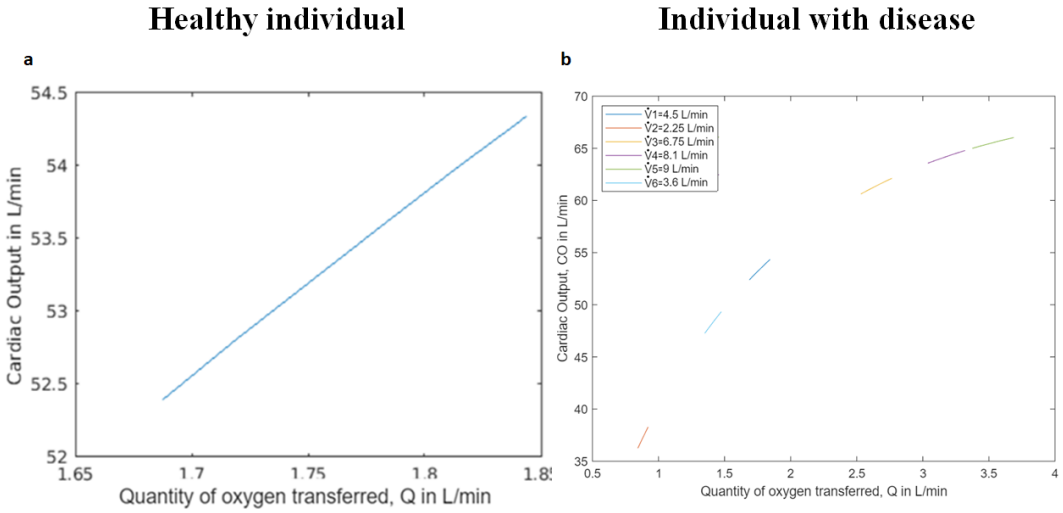

Figure 18. Effects of cerium dioxide nanoparticles on cardiac output: Graph showing the altered effects of oxygen transfer on the cardiac output: lowest cardiac output was observed during the least amount of oxygen transfer which was in turn during the highest amount of cerium dioxide exposure. a) Graph showing the effect of CeO2 nanoparticles on cardiac output in healthy individual b) Graph showing effect of cerium dioxide nanoparticles on the cardiac output for the diseased individual with varied $\dot{V}$, which is calculated with variations in number of breaths per minute

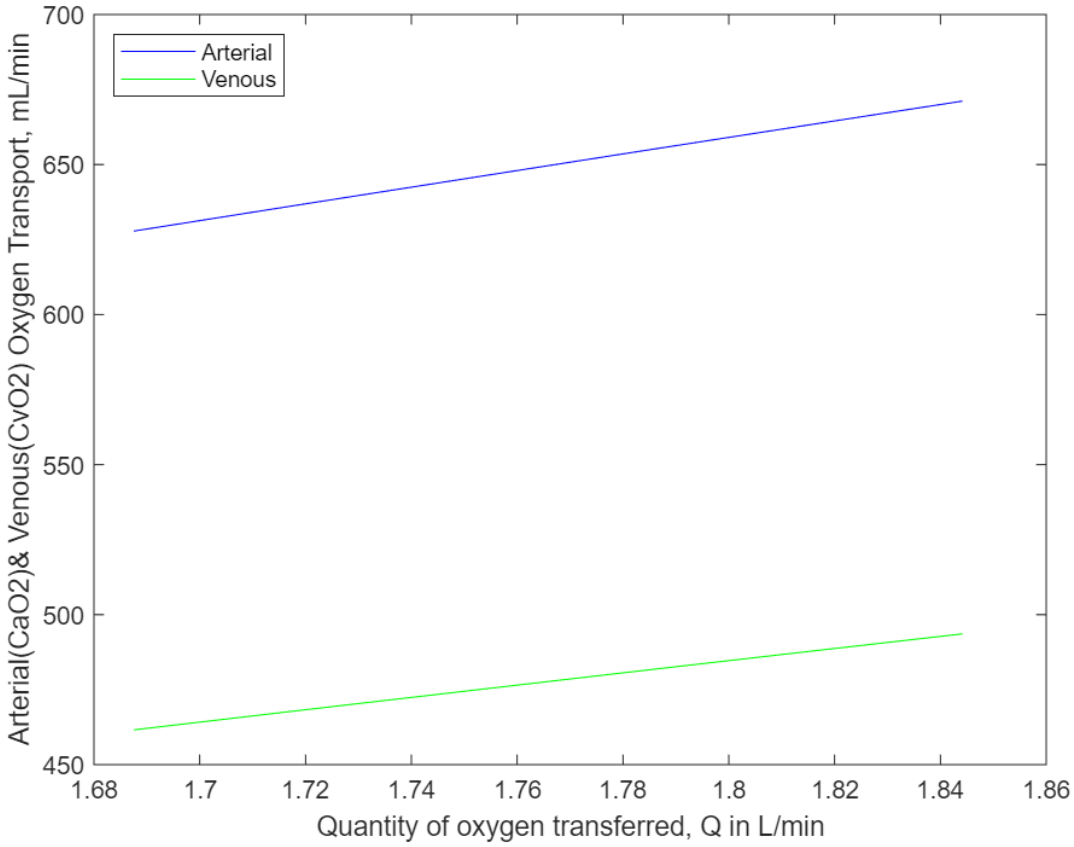

Figure 19. Effects of oxygen transfer after cerium dioxide exposure on arterial and venous oxygen transport: the oxygen volume showed deviations from that observed in normal individual in arterial and venous oxygen transport

Cardiac output, oxygen transport and delivery are all interrelated. All these effects primarily cause a reduction in the oxygen delivery which might result in the clinical conditions, like a decrease in the cardiac output will cause cardiac shock, reduction in metabolic rate and ventricular dysfunction etc. These modeling techniques are the prior analytical methods to determine the effects of nanoparticles. a deeper understanding can however be obtained through animal studies following regulatory guidelines.

CHAPTER V

IN-VITRO MODELING OF ALVEOLO-CAPILLARY BARRIER

5.1. Introduction

As discussed before, cerium dioxide nanoparticles released into environment on their use as diesel fuel additive find their entry into the body primarily through the respiratory system via inhalation mechanism. These nanoparticles tend to move down the respiratory tract deeper into the alveoli. The fate of the cerium dioxide nanoparticles hence starts at the mucociliary clearance absorption of the lungs. These nanoparticles have shown to cross the alveolo-capillary barrier finding entry into different body organs through the systemic circulation. The different toxicities of various nanoparticles in similar size based on the fact of their entry into extra pulmonary organs has been discussed in chapter 1. Alveoli are the main functional pulmonary units of the lungs.

Alveoli and systemic circulation are separated through the alveolo-capillary barrier also termed as air-blood barrier. This barrier is a tight semi-permeable membrane made up of AT-I or alveolar epithelial cell type 1 and AT-II which are the surfactant producing cells[56]. The upper part of the membrane contains a macrophage layer and the basement membrane covered with endothelial cells. This barrier helps in controlling the movement of foreign particles. Cerium dioxide nanoparticles used in the study are of the range 15-30nm. The nanoparticles of the similar size range were known to enter the systemic

circulation and overcoming the clearance mechanisms of alveolar macrophages as discussed in chapter 1, taking this literature fact into consideration, the cerium dioxide nanoparticles will have a greater chance to enter the systemic circulation by crossing the air-blood barrier. To study the effects of cerium dioxide nanoparticles on the air-blood barrier, we aimed at developing the functional air-blood barrier similar to that observed in humans and exposed the barrier to cerium dioxide nanoparticles. The effects were analyzed using confocal microscopy and by barrier electrical resistance measurements also termed as transepithelial/endothelial electrical resistance (TEER). These resistance measurements were taken on the final day without disturbing the setup by only changing the media on alternative days through the 12-day experiment period and the measurements were also taken on the alternative days in another experiment to determine the changes in air-blood barrier formation throughout the experiment period.

In-vitro studies on pulmonary epithelial and endothelial cell lines using different assays provided the preliminary data on cerium dioxide nanoparticle toxicity. These nanoparticles proved to damage the epithelial and endothelial cells. Hence, the effects were determined using co-culture setup which was confirmed using quantitative TEER measurements and by means of confocal microscopy analysis with the membrane tagged using ZO-1 marker.

5.2. Materials and Methods

For the co-culture setup, tissue culture plates treated with polycarbonate membrane polystyrene plates with sizes 0.4µm and 3µm having a diameter of 6.5mm were obtained from Costar Incorporated/life sciences, New York, USA.

5.2.1. A549 Epithelial Monoculture

For the A549 lung epithelial cell line monocultures, cells were plated on 24-well sized transwell permeable inserts at a cell density of 6600 cells ($2x10^4$cells per cm^2) per insert. The cells were plated onto both the 3.0µm pore size and 0.4µm pore size having a surface area of $0.33cm^2$. The apical compartment of transwell insert was filled with 190µl of F12k A549 cell culture media supplemented with serum and antibiotics containing epithelial cells. The basolateral compartment of the inserts was filled with 600µl of the epithelial cell complete medium. The cells were maintained and cultured under submerged conditions for three days for growth. After three days, fresh media was changed on every alternative day throughout the experimental period. For the air-liquid interface setup, the apical pole of the insert media was removed and only the media in the basolateral membrane was changed with fresh media.

5.2.2. EA.hy926 Endothelial Monoculture

For plating endothelial cell line monocultures, the cells were seeded on the basal side of the transwell insert at a cell density of 16,500 cells per insert ($5x10^4$ cells per cm^2) suspended in endothelial cell complete medium. The basal part of the insert was filled with 600µl of endothelial complete media and the apical part with 190µl of A549 F12k cell

culture media. The inserts and the wells of the transwell plates were replaced with fresh endothelial and epithelial media every alternative day throughout the experimental period.

5.2.3. Co-culture Setup

Co-culture setup for the development of in-vitro air-blood barrier was experimentally done by plating the endothelial EA.hy926 cell lines (16,500 cells per insert) suspended in 600µl complete media in the basal part of the insert and on the apical part with A549 epithelial cell lines (6600 cells per insert) suspended in 190µl complete media in the transwell plates of both 0.4µm and 3µm pore sizes.

The co-culture setup was done the same way for both the confocal microscopy and barrier resistance measurements. The cells in the co-cultures were allowed to reach confluency by incubating them at 37^0C and 5% carbon dioxide for three days and from the fourth day, the media was removed and replaced with fresh media every alternative day until analysis.

A549 epithelial cell lines do not form the tight junctions, in order to develop the tight junctions, dexamethasone was added which is known to aid in the formation of tight junctions between the cells. In order to obtain the differential barrier formation analysis, varied concentrations of 1µM and 2µM were added to the co-cultures and A549 monocultures. Dexamethasone was added on the fourth day during replacement of the fresh media onto the apical part of the transwell insert.

5.2.4. Co-culture Confocal Microscopy Analysis

For the confocal microscopy analysis, on the final day, the epithelial and endothelial media from the apical and basal side of the inserts of the transwell plates was removed and washed thrice with 1X PBS. The membranes were carefully cut and kept in petri dishes. The membranes were then treated with 4% paraformaldehyde enough to cover the membranes and incubated for 40 minutes, followed by washing the membranes thrice with 1X PBS. Blocking was done using PBT solution and incubated for 1 hour. ZO-1 antibody with a dilution of 1:500 was added to the membranes and incubated for 30 minutes. The membranes were then washed with 1XPBS thrice and removed, followed by staining with actin green (incubated for 1 hour) and nublue (incubated for 10 minutes) dyes for staining the cytoskeleton and nucleus. The membranes were then incubated with the donkey anti-mouse Cy3 secondary antibody at a dilution of 1:2000 for 30 minutes. The membranes were thoroughly washed with 1X PBS for three times. The membranes were kept on the rectangular glass cover slips. A drop of mounting media was added and covered with another glass cover slip. The samples were left overnight in dark for drying.

5.2.5. TEER Measurements

Electrical resistance measurements were done using EVOM2 voltammeter (World Precision Instruments, Berlin, Germany). The instrument is equipped with STX2 electrode, which were placed in the upper and lower chambers of the co-culture plates to measure the electrical resistance across the barrier. Resistance was measured in terms of $\Omega.cm^2$. Calculations were made by subtracting the blank resistance measurement (transwell membrane without the cells) multiplied by the area of monolayer (0.33 cm^2). The TEER

analysis was done in two forms: measurements taken directly on the final day and measurements taken on the alternative days before replacing the media with fresh epithelial and endothelial media.

5.3. Results and Discussion

5.3.1. Barrier Tight Junction Determination using ZO-1 Marker Through Confocal Microscopy

Confocal microscopy analysis was performed for the co-culture membrane samples prepared after the final day. The barrier should be tight enough to prevent the entry of foreign particles into the systemic circulation. The experiments were performed to develop this barrier in-vitro using co-culture setup. Figure 20 shows the confocal images for the A549 epithelial and EA.hy926 endothelial cell line monocultures along with the air-liquid interface. In-order to obtain a clear image analysis, the cells were fixed using ZO-1 marker which is a membrane protein that enhances the formation of tight junction barriers. A549 monoculture did not show the formation of tight junction whereas EA.hy926 formed the tight junction and hence did not require any dexamethasone treatment confirmed through resistance measurements on both the 0.4µm and 3µm pore sized transwell plates.

A549 epithelial monocultures were hence treated with 1µM and 2µM dexamethasone to enhance the formation of tight junctions. Figure 21 shows the confocal images for the A549 monocultures with and without dexamethasone treatment. As seen in the images, the barrier formation increased with the addition of dexamethasone.

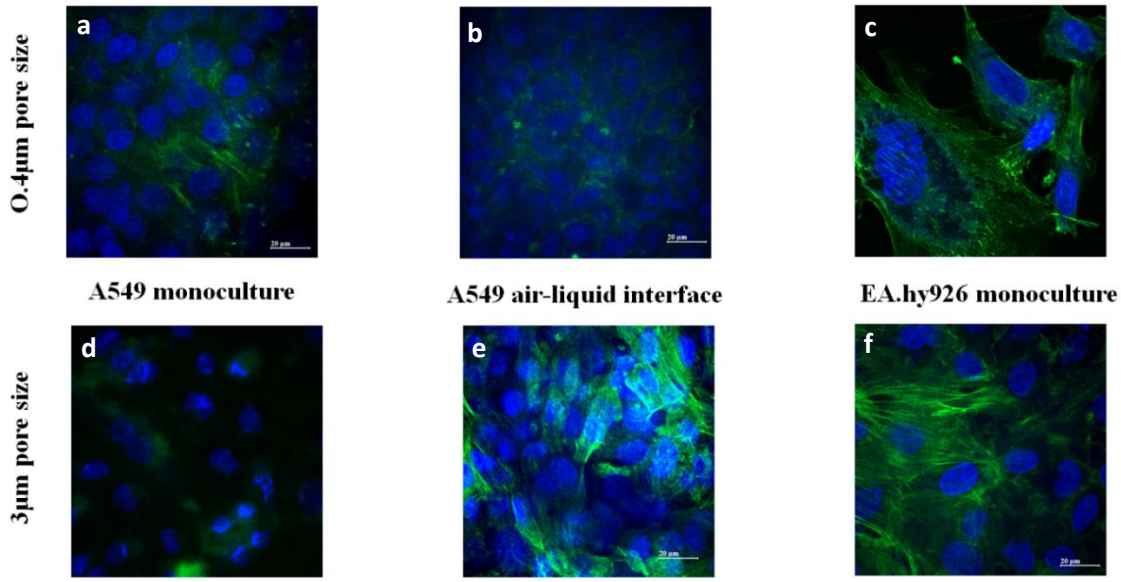

Figure 20. Confocal microscopy of epithelial and endothelial cell line monocultures: Confocal microscopy analysis of A549 epithelial and EA.hy926 endothelial cell line monocultures cultured on 0.4µm and 3µm pore size transwell plates: a, b and c images showing A549 monoculture, A549 air-liquid interface and EA.hy926 monocultures on 0.4µm pore sizes respectively, d, e and f showing A549 monoculture, A549 air-liquid interface and EA.hy926 monoculture on 3µm pore size respectively.

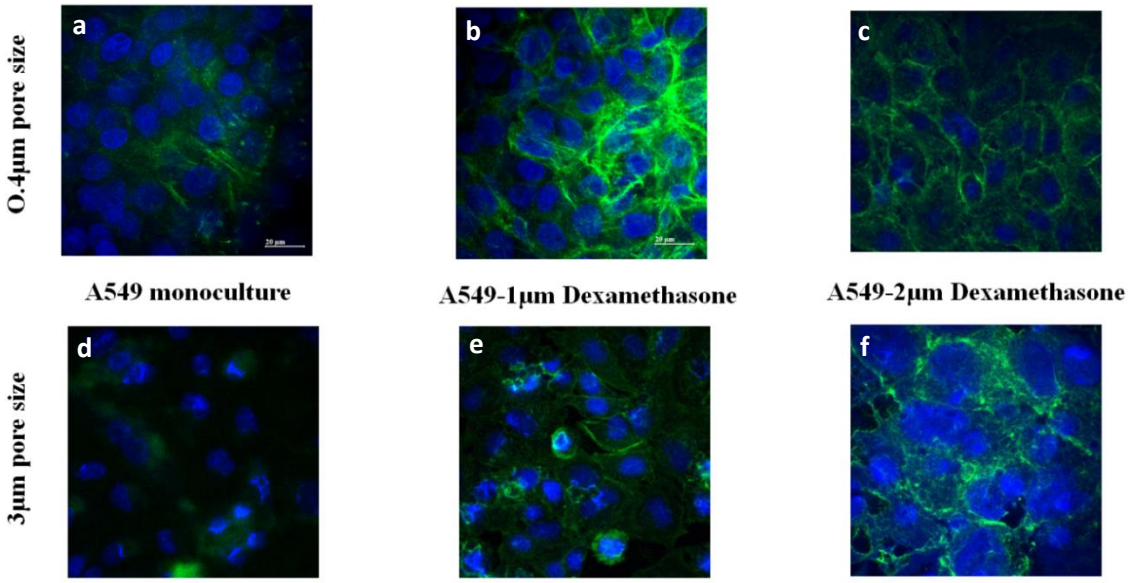

Figure 21. Confocal microscopy of epithelial monocultures after dexamethasone treatment: Confocal microscopy images showing comparative analysis of A549 monocultures with and without dexamethasone treatment with varied concentrations on 0.4µm and 3µm pore sized transwell plates: a, b and c are on 0.4µm transwell plates; d, e and f are on 3µm transwell plates; a) and d) A549 monoculture which showed little or no junctions b) and e) A549 monoculture after treatment with 1µM dexamethasone treatment showed improvement in junction formation c) and f) A549 monocultures after treatment with 2µM dexamethasone showed more improvement in the formation of junctions compared to 1µM dexamethasone treatment.

A549/EA.hy926 co-cultures were shown in figure 22. Co-cultures of both pore sizes did not show discrete formation of barriers however dexamethasone treatment with increasing concentration had shown to increase the tightness of the barrier and hence the discrete barriers can be seen in the images c and f.

Separate plates were seeded and exposed with cerium dioxide nanoparticles at a concentration of 100µg/ml in order to visually analyze the effects on the barrier integrity.

On the final day, the co-cultures treated with 2µM dexamethasone were exposed to cerium dioxide nanoparticles and incubated for 6 hours. In figure 23, a and c images are used for comparative analysis to show the effects of nanoparticles on the barrier. Images b and d shows that the ceria nanoparticles showed disruption in the barrier formed which is confirmed further using TEER measurement values.

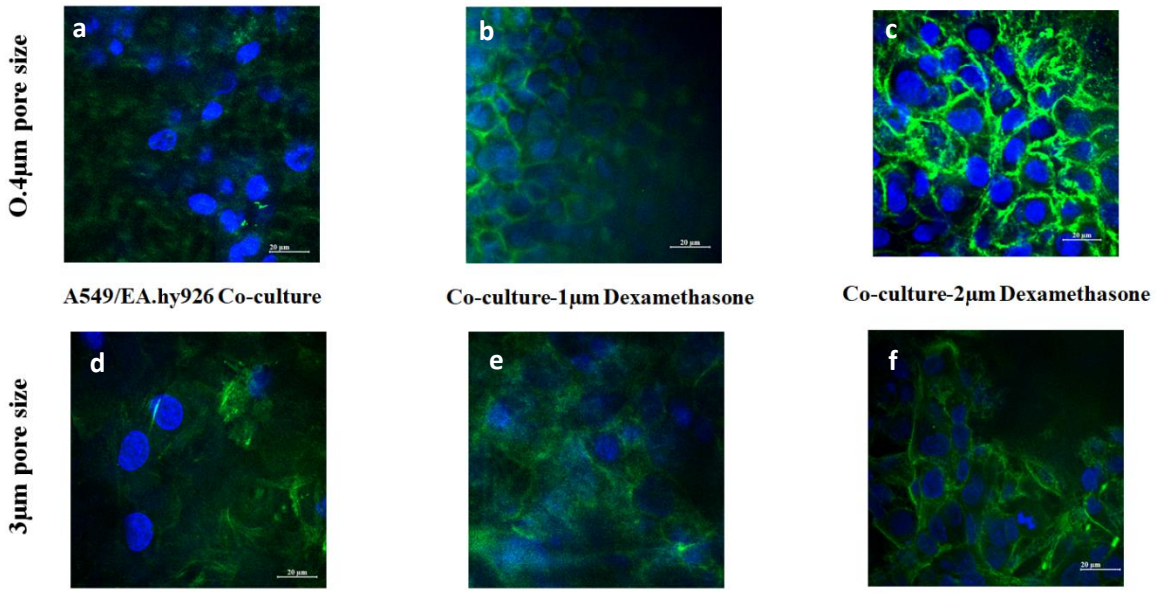

Figure 22. Confocal microscopy of co-cultures with and without dexamethasone treatment: Confocal microscopy analysis of A549/EA.hy926 co-cultures on 0.4µm and 3µm pore sized transwell plates with and without dexamethasone treatment: a, b and c are on 0.4µm transwell plates; d, e and f are on 3µm transwell plates; a) and d) A549/EA.hy926 co-cultures did not show adequate formation of tight junctions b) and e) A549/EA.hy926 co-cultures treated with 1µM dexamethasone and fixed with zo-1 marker showed an improvement in the formation of tight junctions with an enhancement in the visual analysis of junctions because of zo-1 marker c) and f) A549/EA.hy926 co-cultures treated with 2µM dexamethasone and zo-1 marker showed more improvement in the tight junction formation.

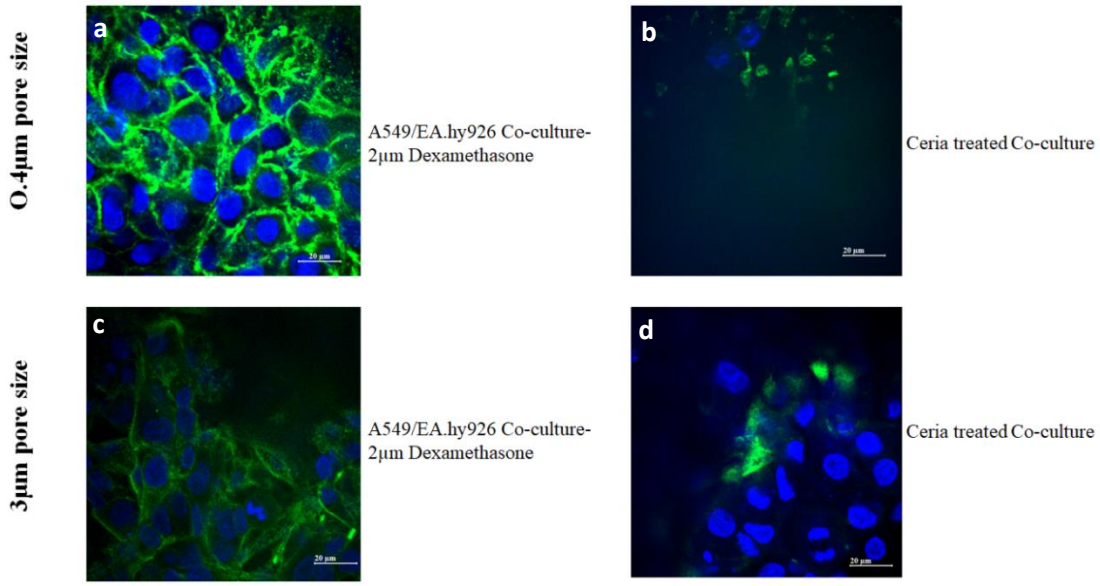

Figure 23. Confocal microscopy analysis of cerium dioxide nanoparticles effects on co-cultures: A549/EA.hy926 co-cultures treated with 2µM dexamethasone exposed to cerium dioxide nanoparticles to study their effects on tight junctions; a) and c) A549/EA.hy926 co-cultures with 2µM dexamethasone are shown as model pictures to visually compare the effects b) and d) A549/EA.hy926 co-cultures with 2µM dexamethasone wells treated with cerium dioxide nanoparticles showed a disruption in the tight junctions formed.

5.3.2. Barrier Electrical Resistance Measurements

5.3.2.1. Transepithelial/endothelial Resistance (TEER) Measurements: Progressive Days

TEER values were measured on alternative days before changing the media every alternative day to monitor the changes in the air-blood barrier formation through para cellular flow across the barrier.

Figure 24 shows the electrical resistance measurements for the A549 monocultures with and without dexamethasone treatment along with EA.hy926 monoculture and A549 air-liquid interface. Figure 24a shows the values for 0.4µm pore sized plates. A549 monoculture showed TEER of 4.1$\Omega.cm^2$ on day 3 which has increased to 28.1 $\Omega.cm^2$. However, treatment with 1µM dexamethasone treatment increased the values to 69 $\Omega.cm^2$ and with 2µM dexamethasone, the value was found to be 97 $\Omega.cm^2$ increasing the tightness of the barrier formed on the final day. Whereas, EA.hy926 monocultures values were found to be 55.8 $\Omega.cm^2$ on the third day which gradually increased to 153.78 $\Omega.cm^2$. For 3µm pore sized plates (figure 24 b), a similar trend in the values were observed however when compared to 0.4µm pore sized plates. A549 monocultures showed resistance values of 2.3 $\Omega.cm^2$ on the third day, which increased to 25.6 $\Omega.cm^2$. Dexamethasone treatment has increased the values from 3.5 and 2.8 $\Omega.cm^2$ to 55 and 89.4 $\Omega.cm^2$ on the final day with 1µM and 2µM dexamethasone treatment respectively. EA.hy926 monocultures values increased from 42.8 to 134.64 $\Omega.cm^2$.

TEER values obtained on the alternative days for A549/EA.hy926 co-cultures with and without dexamethasone treatment were shown in figure 25 for 0.4µm and 3µm pore

sized plates. The values for co-cultures without dexamethasone treatment has shown to increase from 39.6 to 117.7 Ω.cm^2 and 25.6 and 110 Ω.cm^2 in 0.4µm and 3µm pore sized plates. 1µM and 2µM dexamethasone treatment has increased the values to 152 and 221.1 Ω.cm^2 in 0.4µm transwell plate and in 3µm pore size plate, the values increased to 137.1 and 208.3 Ω.cm^2 respectively.

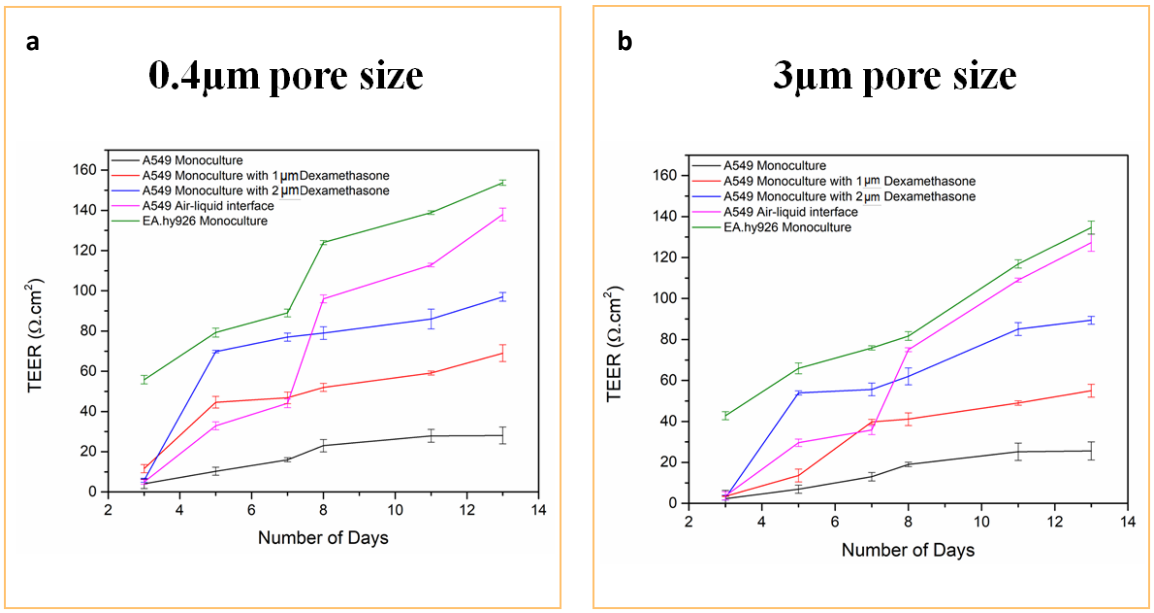

Figure 24. TEER measurements for monocultures with dexamethasone treatment: TEER measurements for monocultures with dexamethasone treatment measured on alternative days to determine the progressive changes in junction formation; a) monocultures cultured on 0.4µm pore sized plates; b) monocultures cultured on 3µm pore sized transwell plates. A549 monocultures showed the least TEER values however after dexamethasone treatment, the resistance values increased representing the tightness of the barrier. EA.hy926 monocultures showed the progressive increase in the resistance values and hence dexamethasone treatment was not required.

The effects of cerium dioxide nanoparticles on the co-cultures with and without dexamethasone treatment were also determined. The co-cultures were exposed to 100µg/ml cerium dioxide nanoparticles for 6 hours and TEER values were measured. Figure 26 shows the effects of the nanoparticles on the co-cultures. As can be seen in the graphs, the treatment has reduced the resistance values from 117.1 to 98 Ω.cm^2, for 1µM dexamethasone treated wells, the resistance values were reduced from 152 to 112 Ω.cm^2 and from 221.6 to 204.6 Ω.cm^2 in 2µM dexamethasone treated wells. Similar trend was observed for 3µm pore sized plates (figure 26b).

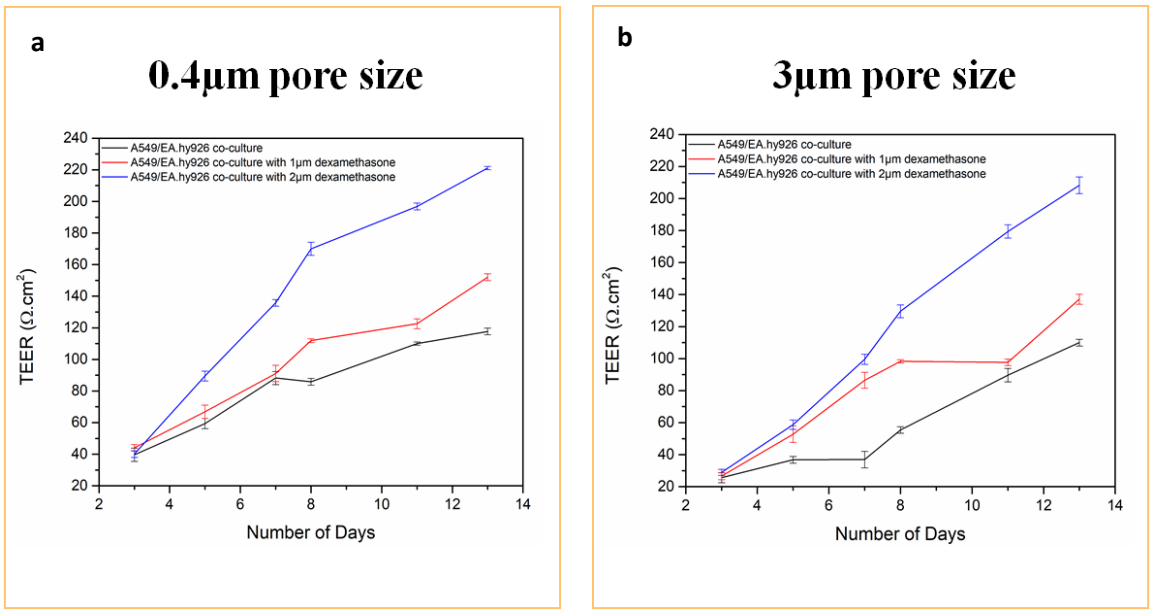

Figure 25. TEER measurements for co-cultures measured on alternative days: TEER measurements for A549/EA.hy926 co-cultures measured on alternative days. a) A549/EA.hy926 co-culture treated with 1µM and 2µM dexamethasone treatment cultured on 0.4µm pore sized transwell plates. b) A549/EA.hy926 resistance progressive values measured on alternative days with and without 1µM and 2µM dexamethasone treatment. The TEER values measured were recorded to be the

lowest in co-cultures, however treatment with dexamethasone increased the resistance values and hence the tight junction formation.

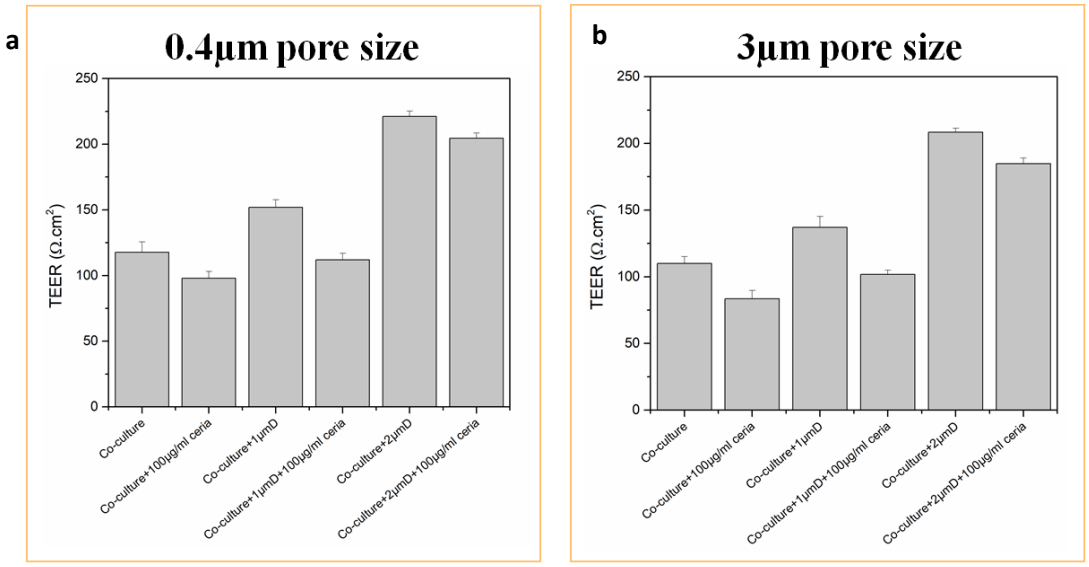

Figure 26. Effects of cerium dioxide nanoparticles on the co-cultures with and without dexamethasone: Graphs showing exposure effects of cerium dioxide nanoparticles on the co-cultures with and without 1µM and 2µM dexamethasone treatment cultured on 0.4µm (a) and 3µm (b) pore size plates. The co-cultures treated with 100µg/ml cerium dioxide nanoparticles showed a reduction in the resistance values when compared to the co-cultures without exposure. A similar trend was observed in the co-cultures with dexamethasone treated with 100µg/ml cerium dioxide nanoparticles.

The results indicated that A549 monocultures required dexamethasone treatment for the formation of tight junctions however EA.hy926 endothelial cell lines formed the tight junctions without treatment with dexamethasone. Cerium dioxide nanoparticles decreased the resistance values in the co-culture which indicated negative effects on the barrier formed. The TEER values depend on passage number of cells, temperature etc. the

conditions should be maintained, and the cells should not be disturbed during the experiment. Hence an experiment was conducted by maintaining the conditions and measuring the TEER values directly on the final day. These experiments were discussed in the following section.

5.3.2.2. Transepithelial/endothelial Resistance (TEER) Measurements: Final Day

TEER measurements were taken on both 0.4µm and 3µm pore size plates. A549 monolayers without dexamethasone treatment have shown a resistance value of 48Ω.cm^2, with 1µM and 2µM dexamethasone concentrations, the TEER values increased to 67 and 152 Ω.cm^2 respectively in 0.4µm pore size whereas in 3µm pore size inserts, the monolayer showed a resistance of 33Ω.cm^2, with 1 µM and 2 µM dexamethasone treatment, the resistance values almost remained the same, 36 and 40Ω.cm^2 respectively. EA.hy926 endothelial monolayers forms the tight junctions as showed in many studies before, however, the resistance values were found to be around 118Ω.cm^2 and 110Ω.cm^2 in 0.4µm and 3µm pore size inserts respectively (figure 27).

A549/Ea.hy926 co-cultured 0.4µm and 3µm pore size inserts (figure 28) showed resistance of 126Ω.cm^2 and 119Ω.cm^2 respectively, whereas the treatment with dexamethasone 1µM and 2µM increased the values to 139Ω.cm^2 and 298Ω.cm^2 in 0.4µm pore size inserts and 129Ω.cm^2 and 286Ω.cm^2 in 3µm pore size inserts. A549 cell lines have been cultured by removing the media in the outer chamber in order to obtain the Air-liquid interface environment and the TEER values were found to be 112Ω.cm^2 and

109Ω.cm^2 in case of 0.4µm and 3µm pore size inserts. The resistance values indicated the formation of tight junctions after treatment with dexamethasone.

100µg/ml cerium dioxide nanoparticles treatment was given in order to determine the toxic effects on the formed air-blood barrier. This concentration was considered depending on the toxicity assay results obtained. Reduced electrical resistance values were obtained in the co-cultures treated with cerium dioxide nanoparticles: in 0.4µm inserts, the values reduced to 62Ω.cm^2 and 60Ω.cm^2 in case of 3µm size inserts. The 0.4µm and 3µm inserts treated with 1µM dexamethasone showed the reduced resistance of 108Ω.cm^2 and 98Ω.cm^2 respectively, whereas the plates treated with 2µM dexamethasone showed the reduced resistance of 119Ω.cm^2 and 110Ω.cm^2 after treatment with cerium dioxide nanoparticles indicating that cerium dioxide nanoparticles caused an injury to the tight barriers.

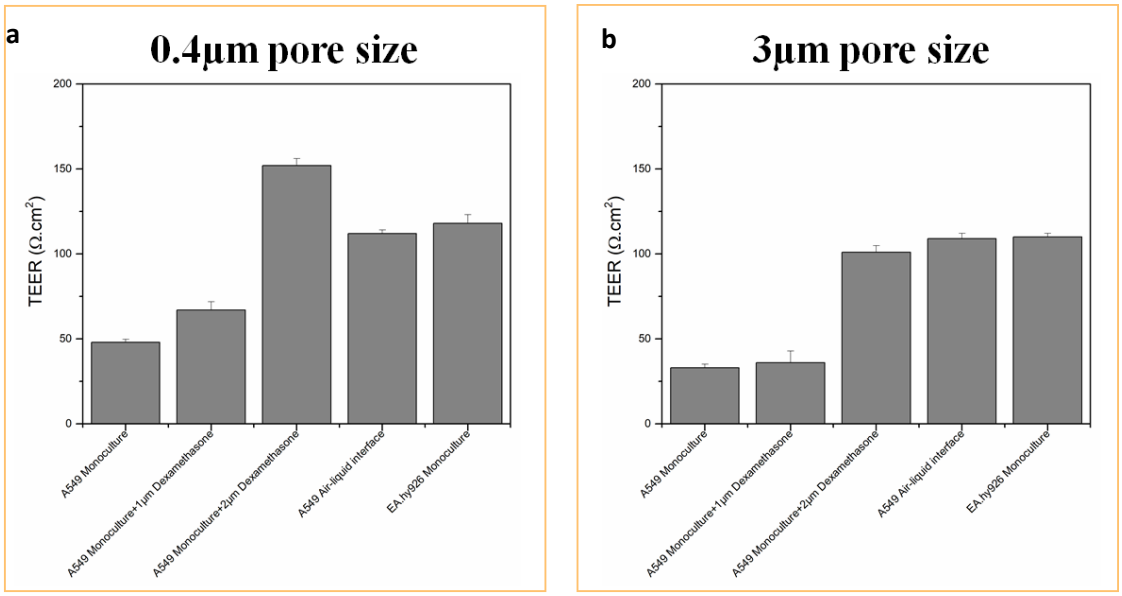

Figure 27. Final day TEER analysis on epithelial monocultures with and without dexamethasone: Graphs showing TEER values measured on final day for A549 cell lines with and without 1µM and 2µM dexamethasone treatment cultured on 0.4µm (a) and 3µm (b) pore sized transwell plates. A549 monocultures in both pore sizes did not show adequate tight junction formation hence lower TEER values were observed. Treatment with dexamethasone increased the resistance values indicating the tight junction formation. EA.hy926 monocultures showed resistance values of 110 and 118Ω.cm^2 in 0.4µm and 3µm pore sizes respectively.

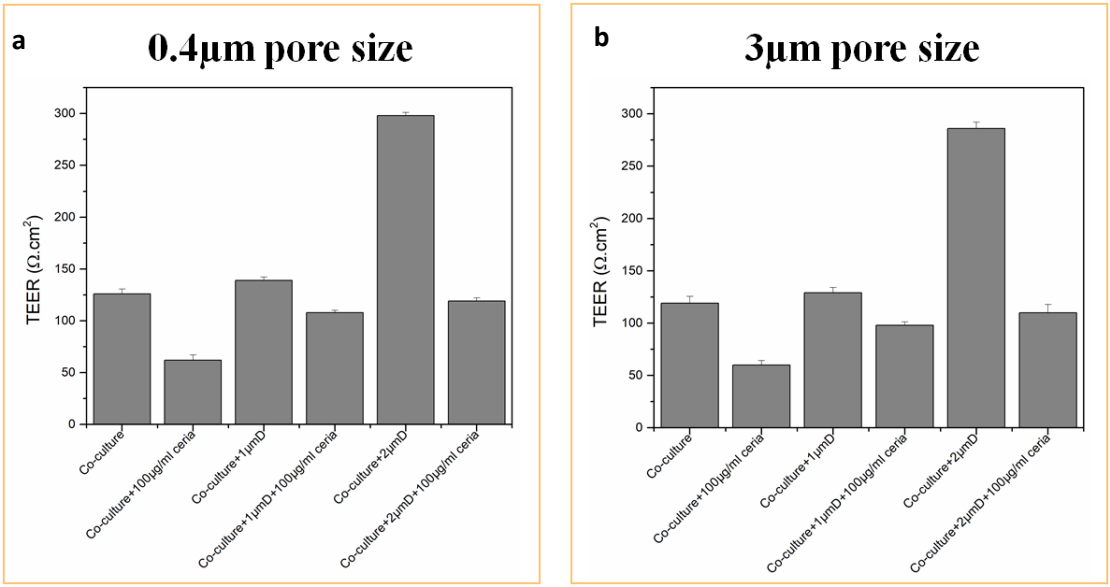

Figure 28. Effects of cerium dioxide nanoparticles on co-cultures with and without dexamethasone: Graphs showing TEER values measured on final day for A549/EA.hy926 co-cultures with and without 1µM and 2µM dexamethasone treatment exposed to 100µg/ml cerium dioxide nanoparticles cultured on 0.4µm (a) and 3µm (b) pore sized transwell plates. The resistance values for co-cultures in both pore sizes were found to be reduced after exposure to cerium dioxide nanoparticles confirming the negative effect on the junctions.

CHAPTER VI

CONCLUSION

Nanotechnology has grown immensely in various industries with many applications allowing the production of materials with scalable new properties. The occupational health and safety has become difficult to predict in the workers working in industries exposed to various engineered nanoparticles making it a predictive concern to see an increased exposure number over the next few years by OHS (Occupational Health and Safety) committee[65]. The current data indicates that the inhaled nanoparticles are insoluble in many applications and can cross the physiological barriers, entering into systemic cirrculation and translocating to different extra-pulmonary organs like heart and brain. The existing knowledge on the safety assessment of engineered nanoparticles is also limited because of the scalable changes in the manufacturing of engineered nanoparticles.

The novel properties which make the nanoparticles attractive in different industrial applications, for example, higher reactivity and the ability to cross cellular membranes, could as well lead to adverse health effects. Prior to performing the cell viability experiments, characterization analysis using different techniques like XRD, FTIR etc., was done in order to confirm the presence of cerium dioxide nanoaparticles. XRD confirmed the presence of cubic flourite crystal structure, raman spectroscopy showed an intense peak with a vibrational mode at $463cm^{-1}$ whereas FT-IR confirmed the presence of CeO_2

showing a peak at 462cm^{-1}. XPS confirmed the presence of Cerium and oxide in the sample and showed the ratios of Ce^{+3} and Ce^{+4} valence states.

The experiments performed, resulted in comparative significant toxicity of 15-30nm cerium dioxide nanoparticles on A549 and EA.hy926 monocultures and co-cultures based on dispersion. The toxicity of Cerium dioxide nanopaticles remain unclear. There were studies which have shown the beneficial aspects of these nanoparticles and there exists many other studies which showed the toxic effects.

The lung cell lines are chosen for the study as inhalation remains the main route of exposure to air-borne ultra fine particles released into the environment through smoke, diesel exhaust etc. Various factors contribute to the lung toxicity through deposition and uptake: size, shape, composition, solubility (dispersion), surface activity and charge. We performed toxicity studies based on dispersion properties.

Tween-80 suspensions showed a greater stability and dispersibility as confirmed by DLS measurements compared to the particles suspended in media directly. Zeta potential values also were higher with tween-80 dispersions compared to the media dispersions. Studies have shown that nanoparticles especially metal oxides, tend to form stronger covalent bonds with proteins and other cellular constituents forming aggregration. Once, aggregated the nanoparticles settle down at the cellular sites and make it impossible for the clearance defence mechanisms to take place. Nanoparticles tend to adsorb to proteins derived from serum added to cell culture medium. Cerium dioxide consists of a higher

protein adsorption capacity. Usually 10% serum will be added to the cell culture media, which should make it sufficient for the formation of secondary particles, aggregates.

The results obtained from cytotoxicity assays, alamar blue and LDH, were in coordinance with theory stated[6, 7]. The percentage toxicity values obtained after 24hour exposure to cerium dioxide nanoparticles dispersed directly in media were 91% with alamar blue where as with tween-80 the toxicity was aorund 70%. With LDH, the toxicity when dispersed in tween-80 was around 40% but in media, the toxicity was doubled. Similar trend was observed in the cells exposed for time periods of 48 and 72 hours.

Cerium dioxide nanoparticles also induced an increased level of ROS production. The production of ROS was observed in a exposure time and concentration dependent manner. These results were only partly consistent with the literature. Studies have shown that these particles did not cause any increased production of ROS [66, 67]. Studies also indicated that the toxicity of the nanoparticles mainly depends on the ratio of 3+/4+ valence states[68]. However, the concentration of these species varied inside and outside of the cell depending on the pH and other cellular parameters.

According to the HEI (Health Effect Institute) reports, cerium dioxide nanoparticle emission from the diesel exhaust will reach up to 22 million pounds annually. Hence, there is a need to evaluate their toxicity in the humans[69]. Once these particles reaches the pulmonary alveolar region, they can be easily translocated into other organs through blood. Endothelial cells forms a monolayer surface which lines the lumen and gives a protective shield functioning as a interface between blood and tissue whereas the epithelial cells will

provide the protection from the outside of the cavity[70]. These two monolayers will connect and form the tight junction which is selectively permeable and controls the transport of harmful particles[71]. Cerium dioxide nanoparticles were released into the environment through diesel exhaust, proving the main route of exposure to be inhalation, if these nanoparticles pass the tight barrier, they can enter the blood stream inducing adverse health effects to various extra pulmonary organs, mainly heart[71].

We established a co-culture system which provides a way to determine the factors affecting the permeability of these nanoparticles in an *in-vitro* setup thereby controlling the experimental conditions and transport factors. Formation of a tight barrier is important to determine the effects after nanoparticle exposure, in order to measure the formation of tight junctions, electrical resistance across the barrier is measured using the TEER instrument which is a quantitative measurement that reflects the paracelllar water flow and the porse size of the tight junction formed[72].

Varied resistance values were obtained in many studies, for instance, Maria.et.al., verified that A549 monoculture showed a TEER value of $9\Omega.cm^2$ and with cocultures the values seemed to remain the same. Even after treatment with dexamethasone, the values increased to $24\Omega.cm^2$[73].

Although there exists clearance mechanims in the body, the alveolar macrophages residing in the alveolar region proved to be inefficient in clearing out the toxic ultra fine particles. A study was conducted on rat lungs, where after 24hr exposure to TiO2 nanoparticles of various sizes, the macrophages failed to engulf and remove the particles

from the body[74]. The data provided showed that cerium dioxide nanoparticles can pass through the tight junctions by injuring the barriers formed which was confirmed using TEER, electrical resistance values.

Our studies showed the comparative toxicity assessment of cerium dioxide nanoparticles using cell toxicity, membrane integrity and ROS assays based on dispersion. The theoretical statement that toxicity decreases based on increased concentration through aggregation confirmed using size and zeta potential measurements has been contradicted in our study. This effect might be because of the saturation of surface states with tween and in case of media samples, because the valence states are uncovered, they might have been inducing the effects by penetrating the cell membrane. Our studies also confirmed the formation of a functional tight air-blood barrier, which remains the main barrier during the transport and exchange of different nanoparticles through the electrical resistance measurements of an *in-vitro* co-culture setup. We also proved the increased cerium dioxide nanoparticle toxicity through reduced electrical resistance values using TEER instrument.

In summary, metal oxide nanoparticles have been increasing used in various industries and their toxic effects were determined in different organs like lungs, heart, skin cells through in-vitro and in-vivo methods. These nanoparticles tend to alter the cellular activity at the genomic level. The toxic effects are based on the nanoparticle dimensions and are closely related to the changes in the surface properties and charges of the nanoparticles. The nanoparticles used in the study are Cerium dioxide nanoparticles belonging to the rare-earth metals. These nanoparticles have two different valence states Ce^{3+} and Ce^{4+}. They tend to react with the molecules within the body and alter the cellular

metabolism. Hence we aimed at studying the reactive oxygen species generation through ROS assay on the A549 epithelial and EA.hy926 endothelial cell lines individually. As mentioned in chapter 1, solubility has been a major concern in using these engineered nanoparticles. They tend to accumulate in different organs and as the clearance mechanisms do not tend to work at the nanoscale range, it is important to determine the effects at the cellular and organ levels. To analyze the solubility and dispersion, we conducted experiments with tween-80 and with complete media.

Inhalation is the main routes of exposure to the cerium dioxide nanoparticles used in this study based on their application as fuel catalysts. We aimed at determining the safety assessment of these nanoparticles on the pulmonary and cardiac cells as respiratory system is the primary route to these nanoparticles. The inhaled gases will be exchanged at the air-blood barrier finding their route into the extra-pulmonary organs through the systemic circulation. In order to understand the effects at the air-blood barrier, we developed an air-blood barrier in-vitro mimicking the functional physiological barrier conditions obersved in-vitro and analyzed the effects of cerium dioxide nanoparticles on the developed barrier integrity using TEER measurements and confocal microscopy analysis using ZO-1 membrane tagging. We also established modeling conditions using in-silico methods to see the effects of cerium dioxide nanoparticles on oxygen transfer changes across the barrier and further aimed at analysing the effects on cardiac cells through cardiac output, oxygen consumption by tissues and blood transport in arteries and veins. The modeling was done using reaction-diffusion model and fick's law. Our models has indicated that cerium dioxide nanoparticles have a negative impact on the air-blood barrier and thus showing

alterations in the different cardiac parameters. Modeling was done with changes in tidal volume to mimic the conditions of individuals with dieases and effects were compared with that of healthy individuals.

All our studies i.e., cytotoxicity assays, membrane integrity assays, reactive oxygen species studies and studies conducted on air-blood barrier through in-vitro co-culture models and in-slico models showed that cerium dioxide nanoparticles are harmful to the human pulmonary and cardiac cells. Cerium dioxide nanoparticles might induce the negative effects on the cells by penetrating into the cell membrane due to the presence of the valence states on their surface. The decrease in toxic effects with tween dispersed samples might be due to the saturation of the valence states upon attachment to tween. Hence, we further hypothesize from our study, that cerium dioxide nanoparticles induce the effects on the cell viability due to the presence of valence states on their surface. A dissolution test and further assessment of toxicity based on this scenario must be perfomed in order to obtain a deeper understanding of the cerium dioxide nanoparticle toxicity.

Due to various regulatory concerns from US FDA and EU, the animals studies were replaced with alternative methods like single cell in-vitro studies, 2D cultures, 3D cultures and in-silico methods. The co-culture studies are a great source to monitor the effects closely to that observed in individuals. However, a careful analysis should still be made concerning the effects of engineered nanoparticles through animal studies. Limited number of animals can be used to determine the effects because of regulatory implications to obtain more thorough analysis of their effects on the individual exposure.

Cerium dioxide nanoparticles are hence released into the environment as pollulants along with other vehicle exhaust emissions considered as polluting the clean air. However, a combination of various pollulants can be used to check the risk wightage of individual gases and combined gases as a whole.

These studies indicate a serious concern on the usage of cerium dioxide nanoparticles as diesel fuel additives and to monitor the concentration ranges in which they are applied making it a precautionary measure. Strict safety assessment and preventive measures must be included by the regulatory authorities to prevent the occupational risk exposure for the workers who manufacture and transform the products to be used in different applications. Though these nanoparticles have many applications, they have the same amount of toxic effects making it a necessity to limit the exposure and protect the worker's and individuals health who have chances for a probable exposure.

REFERENCES

1. Smith, B., *How is Nanotechnology Regulated?* 2018.
2. Cassee, F.R., et al., *Exposure, health and ecological effects review of engineered nanoscale cerium and cerium oxide associated with its use as a fuel additive.* Crit Rev Toxicol, 2011. **41**(3): p. 213-29.
3. Oberdörster, G., et al., *Translocation of Inhaled Ultrafine Particles to the Brain.* Inhalation Toxicology, 2004. **16**(6-7): p. 437-445.
4. Oberdörster, G., et al., *Extrapulmonary translocation of ultrafine carbon particles following whole-body inhalation exposure of rats.* J Toxicol Environ Health A, 2002. **65**(20): p. 1531-43.
5. Lu, X., et al., *Right or left: the role of nanoparticles in pulmonary diseases.* International journal of molecular sciences, 2014. **15**(10): p. 17577-17600.
6. Sukhanova, A., et al., *Dependence of Nanoparticle Toxicity on Their Physical and Chemical Properties.* Nanoscale research letters, 2018. **13**(1): p. 44-44.
7. Shin, S.W., I.H. Song, and S.H. Um, *Role of Physicochemical Properties in Nanoparticle Toxicity.* Nanomaterials (Basel, Switzerland), 2015. **5**(3): p. 1351-1365.
8. Morimoto, Y., et al., *Pulmonary toxicity of well-dispersed cerium oxide nanoparticles following intratracheal instillation and inhalation.* J Nanopart Res, 2015. **17**(11): p. 442.
9. Djurisic, A.B., et al., *Toxicity of metal oxide nanoparticles: mechanisms, characterization, and avoiding experimental artefacts.* Small, 2015. **11**(1): p. 26-44.
10. Calvache-Muñoz, J., F.A. Prado, and J.E. Rodríguez-Páez, *Cerium oxide nanoparticles: Synthesis, characterization and tentative mechanism of particle formation.* Colloids and Surfaces A: Physicochemical and Engineering Aspects, 2017. **529**: p. 146-159.
11. Das, S., et al., *Cerium oxide nanoparticles: applications and prospects in nanomedicine.* Nanomedicine (Lond), 2013. **8**(9): p. 1483-508.
12. Hu, C., et al., *Direct synthesis and structure characterization of ultrafine CeO2 nanoparticles.* Nanotechnology, 2006. **17**(24): p. 5983-5987.
13. *CRC Handbook of Chemistry and Physics, 86th Edition Edited by David R. Lide (National Institute of Standards and Technology). CRC Press (an imprint of Taylor and Francis Group): Boca Raton, FL. 2005. 2544 pp. $125.96. ISBN 0-8493-0486-5.* Journal of the American Chemical Society, 2006. **128**(16): p. 5585-558

14. Nikolaou, K., *Emissions reduction of high and low polluting new technology vehicles equipped with a CeO2 catalytic system.* Science of The Total Environment, 1999. **235**(1): p. 71-76.
15. Morshed, A.H., et al., *Violet/blue emission from epitaxial cerium oxide films on silicon substrates.* Applied Physics Letters, 1997. **70**(13): p. 1647-1649.
16. Feng, X., et al., *Converting Ceria Polyhedral Nanoparticles into Single-Crystal Nanospheres.* Science, 2006. **312**(5779): p. 1504.
17. *Cerium Mischmetal, Cerium Alloys, and Cerium Compounds*, in *Ullmann's Encyclopedia of Industrial Chemistry*.
18. *Cerium and Cerium Compounds*, in *Kirk-Othmer Encyclopedia of Chemical Technology*.
19. Williams, M., *The Merck Index: An Encyclopedia of Chemicals, Drugs, and Biologicals, 15th Edition Edited by M.J. O'Neil , Royal Society of Chemistry, Cambridge, UK ISBN 9781849736701; 2708 pages. April 2013, $150 with 1-year free access to The Merck Index Online.* Drug Development Research, 2013. **74**(5): p. 339-339.
20. Deqing, M., et al., *Role of Cerium Oxide Nanoparticles as Diesel Additives in Combustion Efficiency Improvements and Emission Reduction.* Journal of Energy Engineering, 2015. **142**: p. 04015050.
21. Snow, S.J., et al., *Inhaled diesel emissions generated with cerium oxide nanoparticle fuel additive induce adverse pulmonary and systemic effects.* Toxicol Sci, 2014. **142**(2): p. 403-17.
22. Park, B., et al., *Initial in vitro screening approach to investigate the potential health and environmental hazards of Envirox™ – a nanoparticulate cerium oxide diesel fuel additive.* Particle and Fibre Toxicology, 2007. **4**(1): p. 12.
23. Kristin K. Isaacs1, J.A.R., and Ted B. Martonen3 *Modeling Depostion of Inhaled Particles.* U.S. EPA, National Exposure Research Laboratory, RTP, NC.
24. Watson AY, B.R., Kennedy D, *Biological Disposition of Airborne Particles: Basic Principles and Application to Vehicular Emissions.* Air Pollution, the Automobile, and Public Health. Washington (DC): National Academies Press (US); , 1988.
25. Geiser, M. and W.G. Kreyling, *Deposition and biokinetics of inhaled nanoparticles.* Particle and Fibre Toxicology, 2010. **7**(1): p. 2.
26. Löndahl, J., et al., *Measurement Techniques for Respiratory Tract Deposition of Airborne Nanoparticles: A Critical Review.* Journal of Aerosol Medicine and Pulmonary Drug Delivery, 2013. **27**(4): p. 229-254.
27. Cheng, K.-H., et al., *An Experimental Method for Measuring Aerosol Deposition Efficiency in the Human Oral Airway*. American Industrial Hygiene Association Journal, 1997. **58**(3): p. 207-213.
28. Longest, P.W. and L.T. Holbrook, *In silico models of aerosol delivery to the respiratory tract — Development and applications.* Advanced Drug Delivery Reviews, 2012. **64**(4): p. 296-311.

29. Petosa, A.R., et al., *Aggregation and Deposition of Engineered Nanomaterials in Aquatic Environments: Role of Physicochemical Interactions.* Environmental Science & Technology, 2010. **44**(17): p. 6532-6549.
30. Carvalho, T.C., J.I. Peters, and R.O. Williams, *Influence of particle size on regional lung deposition – What evidence is there?* International Journal of Pharmaceutics, 2011. **406**(1): p. 1-10.
31. Brauer, M., et al., *Air pollution and retained particles in the lung.* Environmental Health Perspectives, 2001. **109**(10): p. 1039-1043.
32. Qiao, H., et al., *The Transport and Deposition of Nanoparticles in Respiratory System by Inhalation.* Journal of Nanomaterials, 2015. **2015**: p. 394507.
33. Oberdörster, G., E. Oberdörster, and J. Oberdörster, *Nanotoxicology: an emerging discipline evolving from studies of ultrafine particles.* Environ Health Perspect, 2005. **113**(7): p. 823-39.
34. Tabata, Y. and Y. Ikada, *Macrophage phagocytosis of biodegradable microspheres composed of L-lactic acid/glycolic acid homo- and copolymers.* J Biomed Mater Res, 1988. **22**(10): p. 837-58.
35. Holsapple, M.P., et al., *Research Strategies for Safety Evaluation of Nanomaterials, Part II: Toxicological and Safety Evaluation of Nanomaterials, Current Challenges and Data Needs.* Toxicological Sciences, 2005. **88**(1): p. 12-17.
36. Nemmar, A., et al., *Ultrafine particles affect experimental thrombosis in an in vivo hamster model.* Am J Respir Crit Care Med, 2002. **166**(7): p. 998-1004.
37. Nemmar, A., et al., *Passage of inhaled particles into the blood circulation in humans.* Circulation, 2002. **105**(4): p. 411-4.
38. Oberdörster, G., *Effects of Ultrafine Particles in the Lung and Potential Relevance to Environmental Particles*, in *Aerosol Inhalation: Recent Research Frontiers: Proceedings of the International Workshop on Aerosol Inhalation, Lung Transport, Deposition and the Relation to the Environment: Recent Research Frontiers, Warsaw, Poland, September 14–16, 1995*, J.C.M. Marijnissen and L. Gradoń, Editors. 1996, Springer Netherlands: Dordrecht. p. 165-173.
39. Park, E.J., et al., *Oxidative stress induced by cerium oxide nanoparticles in cultured BEAS-2B cells.* Toxicology, 2008. **245**(1-2): p. 90-100.
40. Morimoto, Y., et al., *Pulmonary toxicity of well-dispersed cerium oxide nanoparticles following intratracheal instillation and inhalation.* Journal of Nanoparticle Research, 2015. **17**(11): p. 442.
41. Eom, H.-J. and J. Choi, *Oxidative stress of CeO2 nanoparticles via p38-Nrf-2 signaling pathway in human bronchial epithelial cell, Beas-2B.* Toxicology letters, 2009. **187 2**: p. 77-83.
42. McCubbin Donald, R. and A. Delucchi Mark, *The Health Effects of Motor Vehicle-Related Air Pollution*, in *Handbook of Transport and the Environment*, A.H. David and J.B. Kenneth, Editors. 2003, Emerald Group Publishing Limited. p. 411-427.

43. Pekkanen, J., et al., *Particulate air pollution and risk of ST-segment depression during repeated submaximal exercise tests among subjects with coronary heart disease: the Exposure and Risk Assessment for Fine and Ultrafine Particles in Ambient Air (ULTRA) study.* Circulation, 2002. **106**(8): p. 933-8.
44. Rogers, S., et al., *Cerium oxide nanoparticle aggregates affect stress response and function in Caenorhabditis elegans.* SAGE open medicine, 2015. **3**: p. 2050312115575387-2050312115575387.
45. Cho, W.-S., et al., *Metal oxide nanoparticles induce unique inflammatory footprints in the lung: important implications for nanoparticle testing.* Environmental health perspectives, 2010. **118**(12): p. 1699-1706.
46. Ma, J.Y., et al., *Cerium oxide nanoparticle-induced pulmonary inflammation and alveolar macrophage functional change in rats.* Nanotoxicology, 2011. **5**(3): p. 312-325.
47. Palmer, R.J., J.L. Butenhoff, and J.B. Stevens, *Cytotoxicity of the rare earth metals cerium, lanthanum, and neodymium in vitro: comparisons with cadmium in a pulmonary macrophage primary culture system.* Environ Res, 1987. **43**(1): p. 142-56.
48. OECD, *Regulatory Frameworks for Nanotechnology in Foods and Medical Products.* 2013.
49. OECD, *Test No. 403: Acute Inhalation Toxicity*. 2009.
50. Liu, K. and L. Jiang, *Bio-inspired design of multiscale structures for function integration.* Nano Today, 2011. **6**(2): p. 155-175.
51. Martin, S. and B. Maury, *Modeling of the oxygen transfer in the respiratory process∗.* ESAIM: M2AN, 2013. **47**(4): p. 935-960.
52. Poullis, M., *Exploring the boundaries of perfusion. Left field: square tubes and current changes!* The journal of extra-corporeal technology, 2009. **41**(4): p. P21-P24.
53. A., F., *Uber die messung des Blutquantums in den Hertzvent rikeln.* Sitzber Physik Med Ges Wurzburg July 9th: 36, 1870.
54. Geerts, B.F., L.P. Aarts, and J.R. Jansen, *Methods in pharmacology: measurement of cardiac output.* British journal of clinical pharmacology, 2011. **71**(3): p. 316-330.
55. Bengalli, R., et al., *Effect of Nanoparticles and Environmental Particles on a Cocultures Model of the Air-Blood Barrier.* BioMed Research International, 2013. **2013**: p. 801214.
56. Zhao, K.F., et al., *Comparative Toxicity of Nanomaterials to Air-blood Barrier Permeability Using an In Vitro Model.* Biomedical and Environmental Sciences, 2019. **32**(8): p. 602-613.
57. Horváth, L., et al., *Engineering an in vitro air-blood barrier by 3D bioprinting.* Scientific Reports, 2015. **5**(1): p. 7974.

58. Srivastava, M., et al., *Characterizations of in situ grown ceria nanoparticles on reduced graphene oxide as a catalyst for the electrooxidation of hydrazine.* Journal of Materials Chemistry A, 2013. **1**(34): p. 9792-9801.
59. Eriksson, P., et al., *Cerium oxide nanoparticles with antioxidant capabilities and gadolinium integration for MRI contrast enhancement.* Scientific Reports, 2018. **8**(1): p. 6999.
60. Dunnick, K.M., et al., *Evaluation of the effect of valence state on cerium oxide nanoparticle toxicity following intratracheal instillation in rats.* Nanotoxicology, 2016. **10**(7): p. 992-1000.
61. Geiser, M., *Update on macrophage clearance of inhaled micro- and nanoparticles.* J Aerosol Med Pulm Drug Deliv, 2010. **23**(4): p. 207-17.
62. Gustafson, H.H., et al., *Nanoparticle Uptake: The Phagocyte Problem.* Nano today, 2015. **10**(4): p. 487-510.
63. Geiser, M., et al., *The Role of Macrophages in the Clearance of Inhaled Ultrafine Titanium Dioxide Particles.* American Journal of Respiratory Cell and Molecular Biology, 2008. **38**(3): p. 371-376.
64. Zhu, M.-T., et al., *Particokinetics and Extrapulmonary Translocation of Intratracheally Instilled Ferric Oxide Nanoparticles in Rats and the Potential Health Risk Assessment.* Toxicological Sciences, 2008. **107**(2): p. 342-351.
65. Schulte, P.A., et al., *Occupational safety and health criteria for responsible development of nanotechnology.* J Nanopart Res, 2014. **16**(1): p. 2153.
66. Forest, V., et al., *Impact of cerium oxide nanoparticles shape on their in vitro cellular toxicity*. Vol. 38. 2017. 136.
67. Chang, Y.-N., et al., *The Toxic Effects and Mechanisms of CuO and ZnO Nanoparticles.* Materials, 2012. **5**(12): p. 2850-2871.
68. Kumar, A., et al., *Luminescence Properties of Europium-Doped Cerium Oxide Nanoparticles: Role of Vacancy and Oxidation States.* Langmuir, 2009. **25**(18): p. 10998-11007.
69. Institute, H.E., *Evaluation of Human Health Risk from Cerium Added to Diesel Fuel*. 2001: Health Effects Institute.
70. Matter, K. and M.S. Balda, *Functional analysis of tight junctions.* Methods, 2003. **30**(3): p. 228-34.
71. Dekali, S., et al., *Assessment of an in vitro model of pulmonary barrier to study the translocation of nanoparticles.* Toxicol Rep, 2014. **1**: p. 157-171.
72. Huh, D., et al., *Microfabrication of human organs-on-chips.* Nat Protoc, 2013. **8**(11): p. 2135-57.
73. Hermanns, M.I., et al., *Lung epithelial cell lines in coculture with human pulmonary microvascular endothelial cells: development of an alveolo-capillary barrier in vitro.* Lab Invest, 2004. **84**(6): p. 736-52.
74. Oberdörster, G., et al., *Role of the alveolar macrophage in lung injury: studies with ultrafine particles.* Environmental Health Perspectives, 1992. **97**: p. 193-199.